united nations educational, scientific and cultural organization

international atomic energy agency

the
abdus salam
international centre for theoretical physics

Course on "Inverse Methods in Atmospheric Science"
1 - 12 October 2001

301/1332-4

"Numerical Methods for Forward Models"

K. STAMNES
Stevens Institute of Technology
Hoboken,NJ
USA

Please note: These are preliminary notes intended for internal distribution only.

strada costiera, 11 - 34014 trieste italy - tel. +39 0402240111 fax +39 040224163 - sci_info@ictp.trieste.it - www.ictp.trieste.it

Brief Tutorial on Radiative Transfer Modeling

Knut Stamnes

Light and Life Laboratory

Department of Physics & Engineering Physcis

Arthur E. Imperatore School of Sciences Arts

Stevens Institute of Technology

Hoboken, NJ 07030

Light and Life Laboratory STEVENS Institute of Technology

Physical Overview of the Transfer of Solar Radiation in the Atmosphere - Ocean System

Light propagation in the atmosphere-ocean system depends on:

- Atmospheric optical properties such as

=> Absorption by molecules (H_2O, O_3, CO_2, and others)
=> Scattering by atmospheric molecules (Rayleigh scattering)
=> Scattering by aerosols

- Oceanic optical properties such as

=> Absorption by pure water
=> Scattering by density fluctuations (Rayleigh scattering)
=> Absorption by yellow substance or colored dissolved organic matter (CDOM)
=> Scattering and absorption by suspended particles
=> Scattering and absorption by air bubbles in the water column

Light propagation also depends on:

- **Fresnel reflection and transmission through the atmosphere-ocean interface**
- **Scattering by surface roughness (foam, white caps)**

In addition:

- sources of light due to fluorescence and Raman scattering may **(depending on wavelength) contribute to the light field in the ocean.**

Simulation of the solar signal in the atmosphere-ocean system

Physical overview

- Scattering and absorption by aerosol layer
- Scattering and absorption by algae cells
- Scattering and absorption by suspended matter
- Absorption by yellow matter

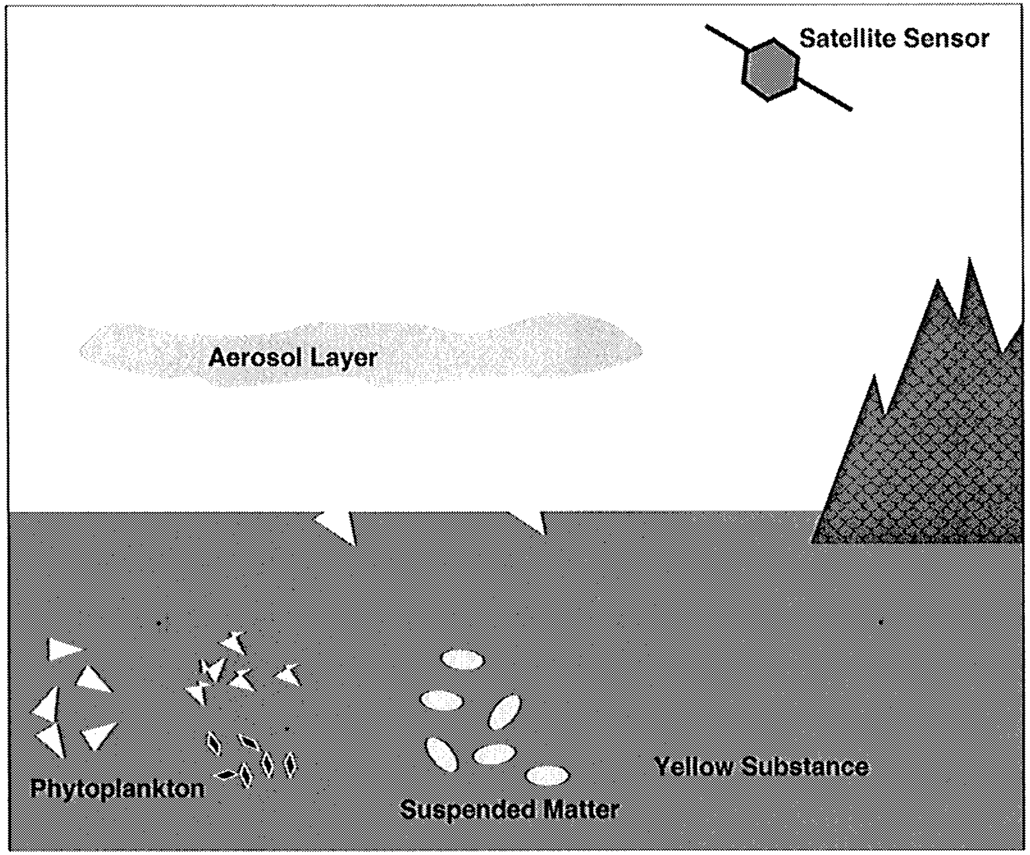

Figure 1: Illustation of Light Propagation In the Atmosphere-Ocean System

Radiative Transfer Modeling

We consider a vertically stratified medium for which the transfer of diffuse radiation is described by the equation of radiative tranfer ($u = \cos\theta$; $\theta =$ polar angle; $\phi =$ azimuthal angle):

$$u\frac{dI(\tau,u,\phi)}{d\tau} = I(\tau,u,\phi) - S(\tau,u,\phi), \tag{1}$$

$$S(\tau,u,\phi) = \frac{a(\tau)}{4\pi}\int_0^{2\pi} d\phi' \int_{-1}^{1} du' p(\tau,u',\phi',u,\phi) I(\tau,u',\phi') + S^*(\tau,u,\phi). \tag{2}$$

For the coupled atmosphere-ocean system, the change in the refractive index across the interface must be accounted for. From elementary optics we know that:

- The refraction across the interface is described by Snells' law
- The reflection and transmission are described by Fresnel's equations
- The downward radiation distributed over 2π steradians in the atmosphere will be restricted to an angular cone less then 2π after being refracted into the ocean (see Figure below).

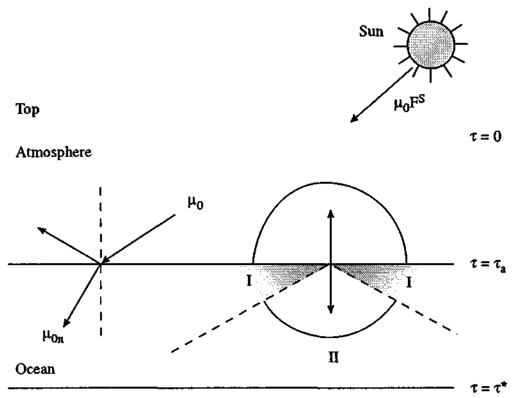

Figure 2: Schematic Illustration of two adjacent media with a flat interface such as the atmosphere overlying a calm ocean.

Definitions:

$$\begin{aligned}
d\tau &= [\alpha(z)+\sigma(z)]\,dz \quad \textbf{optical depth} && (3)\\
\alpha(z) &= \textbf{absorption coefficient } [\mathrm{m}^{-1}] && (4)\\
\sigma(z) &= \textbf{scattering coefficient } [\mathrm{m}^{-1}] && (5)\\
a(z) &= \frac{\sigma(z)}{\alpha(z)+\sigma(z)} \quad \textbf{single scattering albedo} && (6)\\
\alpha(z) &\equiv \sum_i \alpha^i(z) = \sum_i n^i\,\alpha_n^i\,; \qquad \sigma(z) \equiv \sum_i \sigma^i(z) = \sum_i n_i\,\sigma_n^i && (7)\\
\alpha_n^i &= \textbf{absorption cross section } [\mathrm{m}^2] && (8)\\
\sigma_n^i &= \textbf{scattering cross section } [\mathrm{m}^2] && (9)\\
n_i &= \textbf{concentration of } i^{\mathrm{th}} \textbf{ species } [\mathrm{m}^{-3}] && (10)
\end{aligned}$$

Phase function (normalized angular scattering cross section):

$$\begin{aligned}
p(\tau,\cos\Theta) &= p(\tau,u',\phi';u,\phi) = \frac{\sum_i\ \sigma^i(\tau,cos\Theta)}{\sum_i\int_{4\pi} d\ cos\Theta\ \sigma^i(\tau,cos\Theta)/4\pi} = \frac{\sum_i\ \sigma^i(\tau,cos\Theta)}{\sum_i\ \sigma^i(\tau)} = \frac{\sigma(\tau,cos\Theta)}{\sigma(\tau)} && (11)\\
\Theta &= \textbf{scattering angle} && (12)\\
(\theta',\phi') &= \textbf{polar and azimuthal angles } \textit{prior to} \textbf{ scattering} && (13)\\
(\theta,\phi) &= \textbf{polar and azimuthal angles } \textit{after} \textbf{ scattering} && (14)
\end{aligned}$$

These angles are related through the cosine law of spherical geometry:

$$\cos\ \Theta = cos\ \theta'\ cos\theta + sin\ \theta'\ sin\ \theta\ cos(\phi'-\phi). \qquad (15)$$

Factoring out Azimuthal Dependence - 1

- **Expand phase function in Legendre polynomials:**

$$p(\tau, \cos\,\Theta) \;=\; \sum_{l=0}^{2M-1} (2l+1)\chi_l(\tau)\; P_l(\cos\Theta) \tag{16}$$

where $P_l(\cos\Theta)$ is the Legendre polynomial and the expansion coefficients are given by:

$$\chi_l(\tau) \;=\; \frac{1}{2}\int_{-1}^{1} d\;\cos\Theta\; p(\tau, \cos\Theta)\; P_l(\cos\Theta) \tag{17}$$

- **Addition Theorem for Spherical Harmonics:**

$$P_l(cos\Theta) = P_l(u')P_l(u') + 2\sum_{m=1}^{l} \Lambda_m^l(u')\Lambda_l^m(u)\cos m(\phi' - \phi) \tag{18}$$

$$\Lambda_l^m(u) = \left[\frac{(l-m)!}{(l+m)!}\right]^{1/2} P_l^m(u) \tag{19}$$

- **The phase function now becomes:**

$$p(\tau, \cos\;\Theta) = p(u', \phi'; u, \phi) = \sum_{m=0}^{2M-1} (2 - \delta_{0m})\; p^m(u', u)\; cos m(\phi' - \phi)$$

where

$$p^m(u', u) = \sum_{l=m}^{2M-1} (2l+1)\; \chi_l\; \Lambda(u')\; \Lambda(u).$$

Light and Life Laboratory
STEVENS Institute of Technology

Factoring out Azimuthal Dependence - 2

- **Now expand intensity as:**

$$I(\tau, u, \phi) \;=\; \sum_{m=0}^{2N-1} I^m(\tau, u)\; \cos m(\phi_0 - \phi) \tag{20}$$

- **This leads to an equation for each Fourier component:**

$$u\frac{dI^m(\tau, u)}{d\tau} \;=\; I^m(\tau, u) - \frac{a(\tau)}{2}\int_{-1}^{1} p^m(\tau, u', u) I^m(\tau', u) du' \;-\; X_0^m(\tau, u) e^{-\tau/\mu_0} \tag{21}$$

where

$$X_0^m(\tau, u) \;=\; \frac{a(\tau)}{2} F_0(2 - \delta_{0m}) p^m(\tau, \mu_0, u). \tag{22}$$

Light and Life Laboratory STEVENS Institute of Technology

Factoring out Azimuthal Dependence - 3

The Azimuthal Dependence of the Radiative Transfer Equation has been factored out in the sense that:

- The Fourier components are entirely uncoupled
- Independent solutions to Eq. (21) for each m give the azimuthal components
- The sum in Eq. (20) then yields the complete azimuthal dependence of the radiance

Note also:

- Azimuthal dependence can be traced to the boundary conditions:
- **If there is no azimuth-dependent beam source or reflection at either boundary, the sum in Eq. (20) reduces to the $m = 0$ term, the angles μ_0 and ϕ_0 are irrelevant, and there is no azimuthal dependence of the diffuse radiance.**

Henyey-Greenstein Phase Function

- **This synthetic one-parameter phase function is given by:**

$$P_{HG}(cos\Theta) = \frac{1-g^2}{(1+g^2-2g\ \cos\Theta)^{3/2}} \tag{23}$$

where the parameter g is the asymmetry factor:

$$g = \chi_1. \tag{24}$$

- **Legendre polynomial expansion coefficients of the Henyey-Greenstein phase function:**

$$\chi_l = (g)^l \tag{25}$$

- **This property explains its popularity because there is no need to compute Legendre polynomial expansion coefficients!**

Note that:

- $g = 0$ for isotropic scattering
- $g = 1$ for complete forward scattering
- $g = -1$ for complete backward scattering.

Scaling Transformations

δ - Isotropic Approximation:

$$\hat{p}_{\delta-iso}(u^{'}, u) \equiv \frac{1}{2\pi}\int_0^{2\pi} d\phi \;\; \hat{p}(cos\phi) = 2f\delta(u^{'}, u) + (1-f)$$

leads to

$$u\frac{dI(\hat{\tau}, u)}{d\tau} = I(\tau, u) - \frac{\hat{a}}{2}\int_{-1}^{1} du^{'} I(\hat{\tau}, u^{'})$$

$$d\hat{\tau} \equiv (1 - af)d\tau, \qquad \hat{a} \equiv \frac{(1-f)a}{1-af}$$

Setting $f = \chi_1 = g$ yields: $\quad \hat{\alpha} = \alpha, \qquad \hat{\sigma} = (1-g)\sigma, \qquad \hat{g} = 0.$

δ-Two-Term Approximation:

$$\hat{p}_{\delta-TTA}(u', u) = 2f\delta(u', u) + (1-f)(1 + 3\,\chi_1 u' u)$$

$$\hat{\chi}_1 \equiv \hat{g} = \frac{\chi_1 - f}{1-f} = \frac{g-f}{1-f}$$

Setting $f = \chi_2 = g^2$ yields: $\quad \hat{\alpha} = \alpha, \qquad \hat{\sigma} = (1-g^2)\sigma, \qquad \hat{g} = g/(1+g).$

These approximations are very popular in the diffusion approximation.

Discrete-Ordinate-Approximation

Since azimuthal components in Eq. (20) are uncoupled, we may focus on azimuthally-averaged radiance obtained by setting m = 0. We obtain a pair of coupled *Integro-differential* equations:

$$\mu\frac{dI^+(\tau,\mu)}{d\tau} = I^+(\tau,\mu) - \frac{a}{2}\int_0^1 d\mu' p(\mu',\mu)I^+(\tau,\mu') - \frac{a}{2}\int_0^1 d\mu' p(-\mu',\mu)I^-(\tau,\mu') - X_0^+ e^{-\tau/\mu_0} \quad (26)$$

$$-\mu\frac{dI^-(\tau,\mu)}{d\tau} = I^-(\tau,\mu) - \frac{a}{2}\int_0^1 d\mu' p(\mu',-\mu)I^+(\tau,\mu') - \frac{a}{2}\int_0^1 d\mu' p(-\mu',-\mu)I^-(\tau,\mu') - X_0^- e^{-\tau/\mu_0} \quad (27)$$

where $(\mu = |\mu|)$

$$p(\mu',\mu) = \sum_{l=0}^{2N-1}(2l+1)\chi_l P_l(\mu')P_l(\mu); \qquad X_0^\pm \equiv X_0(\pm\mu) = \frac{a}{4\pi}F_0 p(-\mu_0,\pm\mu)$$

Discrete-ordinate approximation:

- ***Replace integrals in equations above by quadrature sums, thereby transforming:***
- ***pair of coupled integro-differential equations into a system of coupled differential equations:***

$$\mu_i\frac{dI^+(\tau,\mu_i)}{d\tau} = I^+(\tau,\mu_i) - \frac{a}{2}\sum_{j=1}^{N} w_j p(\mu_j,\mu_i)I^+(\tau,\mu_j) - \frac{a}{2}\sum_{j=1}^{N} w_j p(-\mu_j,\mu_i)I^-(\tau,\mu_j) - X_{0i}^+ e^{-\tau/\mu_0} \quad (28)$$

$$-\mu_i\frac{dI^-(\tau,\mu_i)}{d\tau} = I^-(\tau,\mu_i) - \frac{a}{2}\sum_{j=1}^{N} w_j p(\mu_j,-\mu_i)I^+(\tau,\mu_j) - \frac{a}{2}\sum_{j=1}^{N} w_j p(-\mu_j,-\mu_i)I^-(\tau,\mu_j) - X_{0i}^- e^{-\tau/\mu_0} \quad (29)$$

Light and Life Laboratory
STEVENS Institute of Technology

Photolysis Rate

In atmospheric photochemistry

- **the Photolysis Rate Coefficient is defined as the local rate (per molecule) of a photoabsorption event.**

- the photolysis rate coefficient for the photodissociation of a particular species of concentration n_i is expressed as follows:

$$J_i \equiv \int_{\nu_c}^{\infty} d\nu \, 4\pi \left(\bar{I}_\nu / h\nu\right) n_i \, \alpha_n^i(\nu) \, \eta^i(\nu) \qquad [s^{-1}].$$

Here:

- $\alpha_n^i(\nu)$ **is the photoabsorption cross section,**
- $\eta^i(\nu)$ $(0 \leq \eta^i \leq 1)$, is the *quantum yield* or efficiency by which the absorbed radiative energy produces the photodissociation,
- ν_c **is the minimum frequency corresponding to the threshold energy for the photoabsorption,** $\bar{I}$ **is the mean intensity, and**
- $4\pi\bar{I}_\nu/h\nu$ is the density of photons at a given frequency.

Photochemists use the term actinic flux for the quantity $4\pi\bar{I}_\nu$. **Optical oceanographers call this quantity the** scalar irradiance.

Light and Life Laboratory STEVENS Institute of Technology

Biological Dose Rate

The rate at which a surface receives radiative energy capable of initiating certain biological processes is obtained by:

- **weighting the received radiation by a specific spectral function A(ν) < 1 called the action spectrum, which**
- gives the efficiency of a particular process, for example, the UV 'kill-rate'.
- **The rate at which a flat surface is 'exposed' is called the Dose Rate:**

$$D \equiv \int_0^\infty d\nu A(\nu) F_\nu^- \qquad [W \cdot m^{-2}]$$

where:

- F_ν^- is the incident irradiance.
- **The radiation dose is defined to be the total time-integrated amount of energy received (usually over one day)** $\int dt D(t)$.

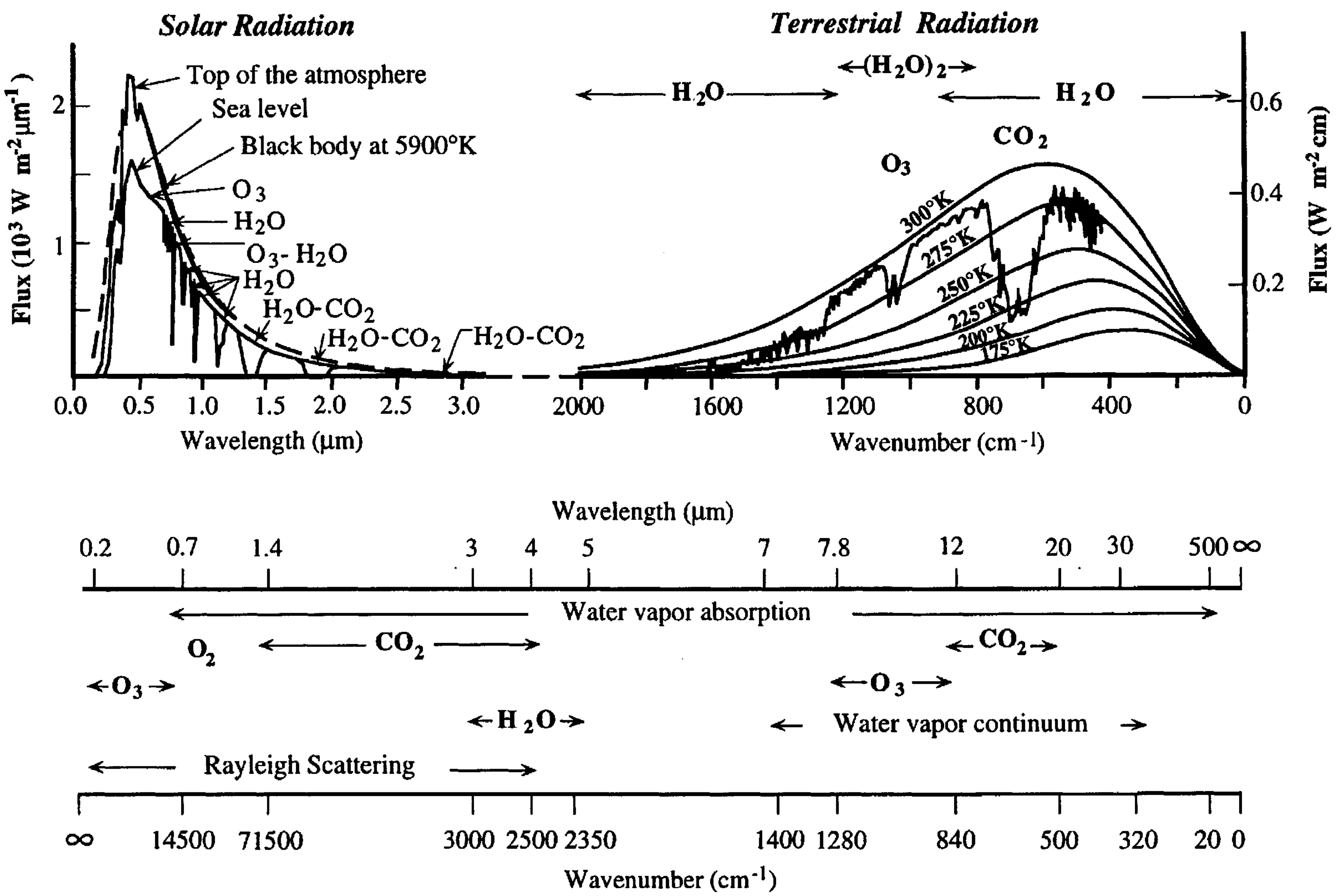

Figure 3: Spectral distribution of solar (short-wave) and terrestrial (long-wave) radiation fields. Also shown are the approximate shapes and positions of the scattering and absorption features of the Earth's atmosphere.

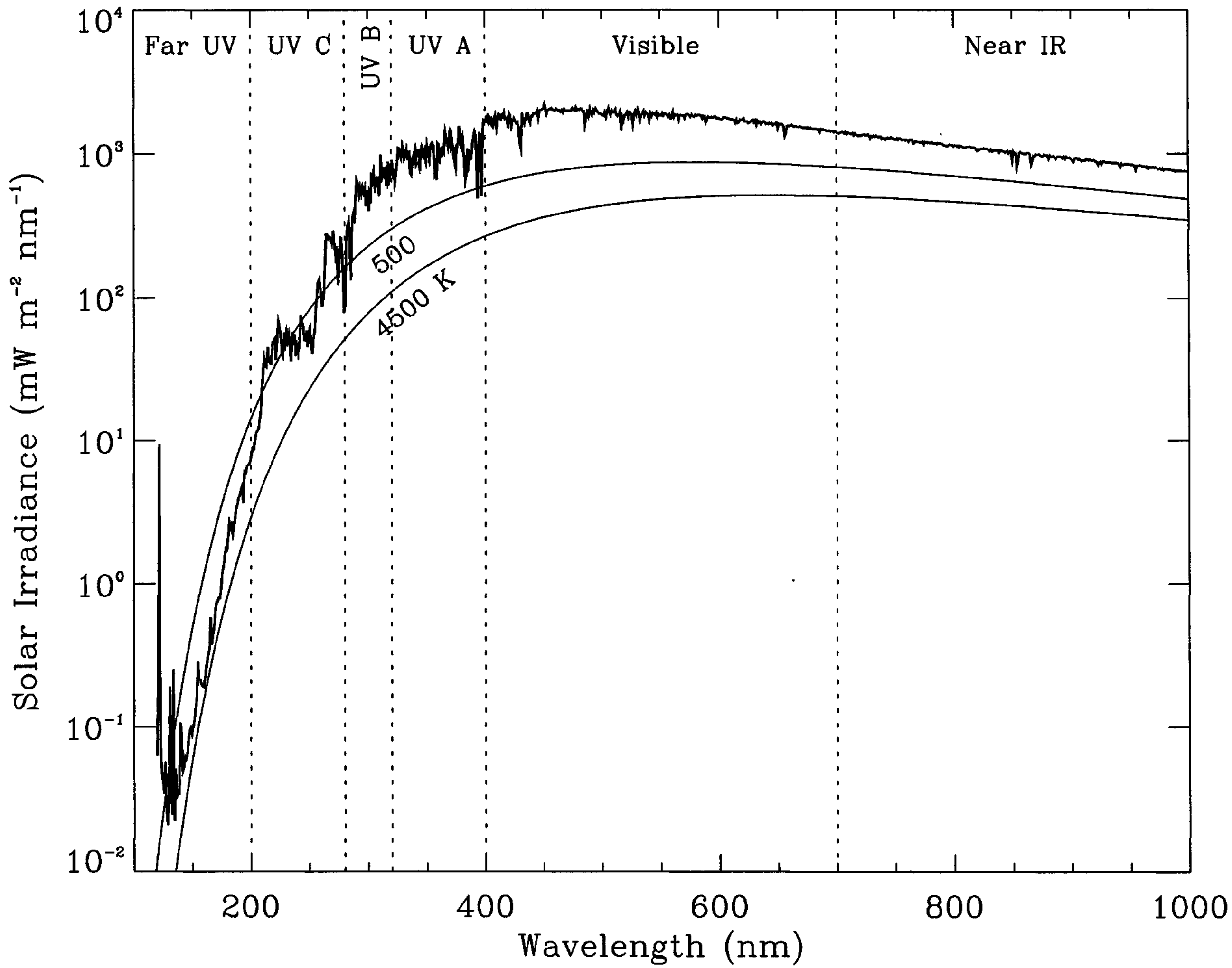

Figure 4: Extraterrestrial solar irradiance, measured by a spectrometer on board an Earth-orbiting satellite. The UV spectrum ($119 < \lambda < 420$ nm) was measured by the SOLSTICE instrument on the UARS satellite (modified from a diagram provided by G. J. Rottmann, private communication, 1995).

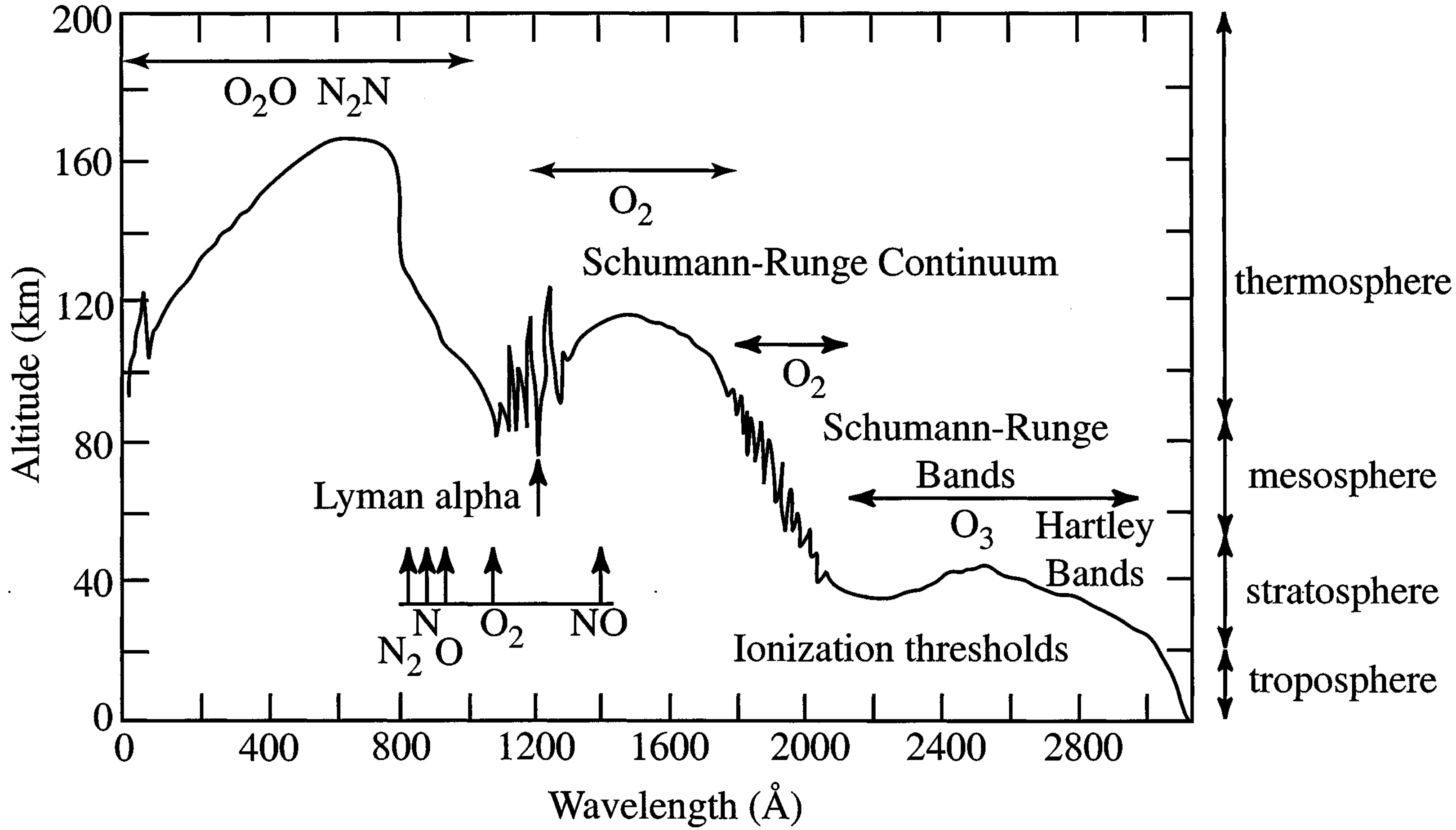

Figure 5: Atmospheric penetration depth versus wavelength. Horizontal arrows indicate the molecule (and band) responsible for absorption in that spectral region. Vertical arrows indicate the ionization thresholds of the various species.

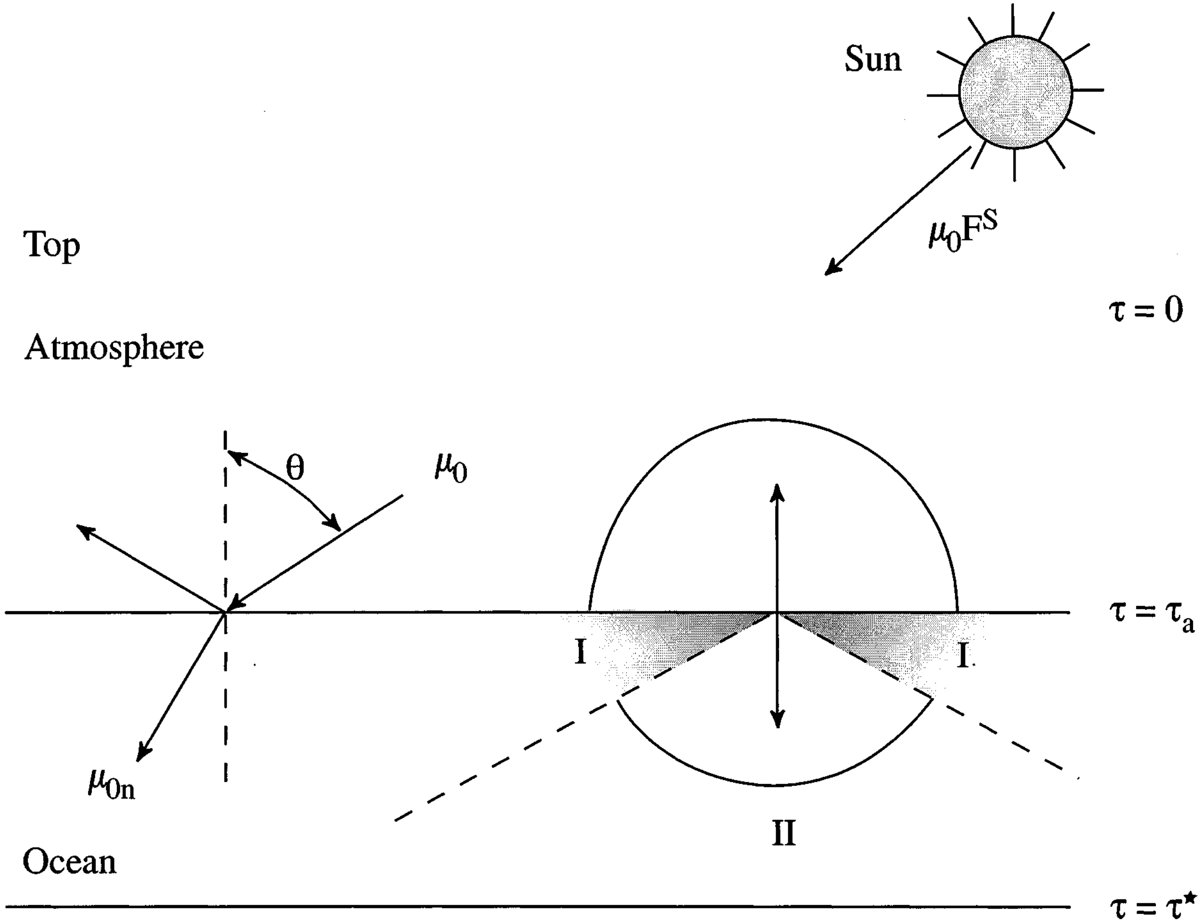

Figure 6: Schematic illustration of two adjacent media with a flat interface such as the atmosphere overlying a calm ocean. The atmosphere has a different index of refraction ($m_r \approx 1$) than the ocean ($m_r = 1.33$). Therefore, radiation in the atmosphere distributed over 2π sr will be confined to a cone less than 2π sr in the ocean (region II). Radiation in the ocean within region I will be totally reflected when striking the interface from below (adapted from Thomas and Stamnes, 1999).

Comparison of DISORT Results with Monte Carlo Simulations

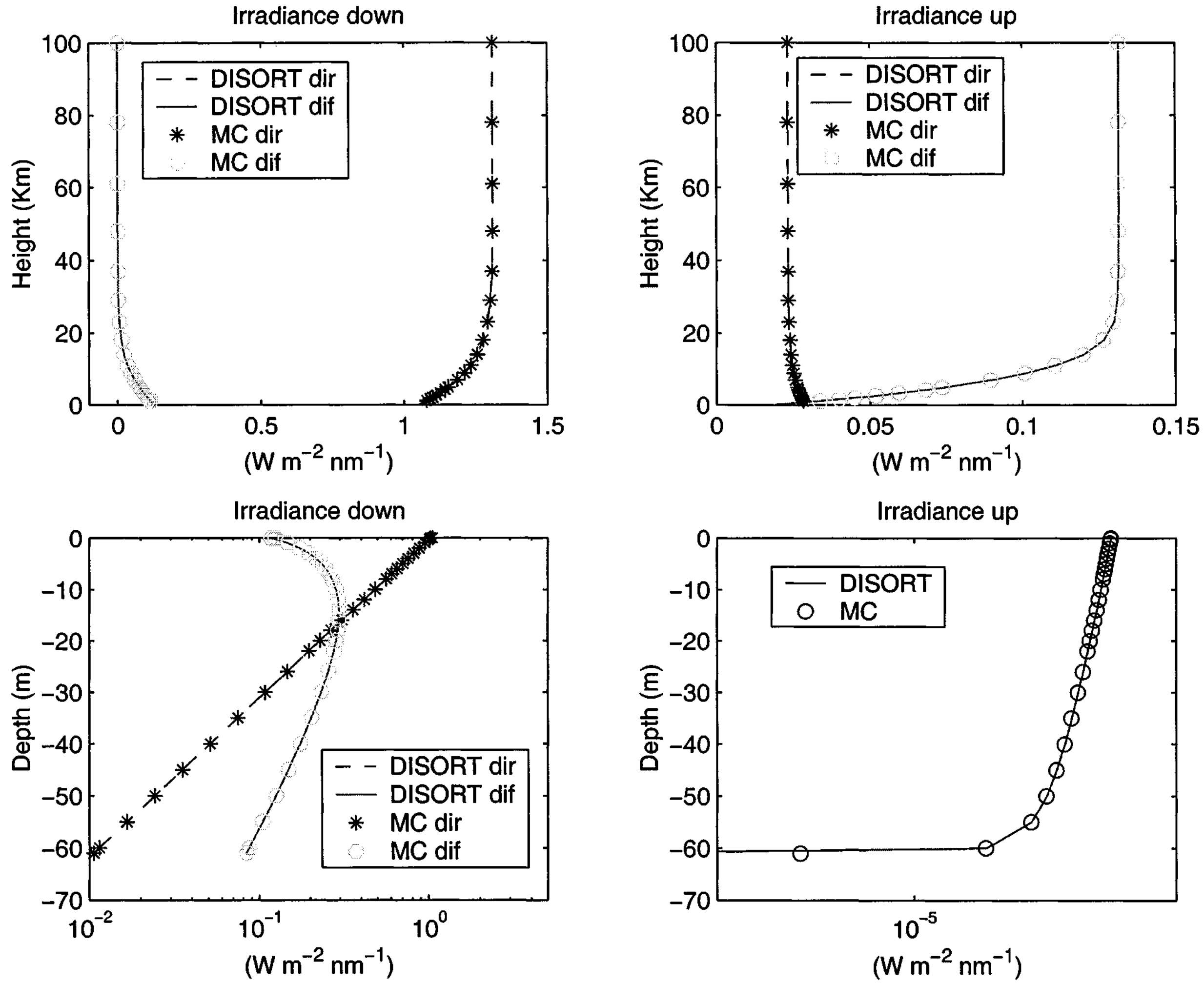

Figure 7: Comparison of DISORT and Monte Carlo Results for the Coupled Atmopshere Ocean System. The Monte Carlo Computations are due to K. I. Gjerstad, University of Bergen.

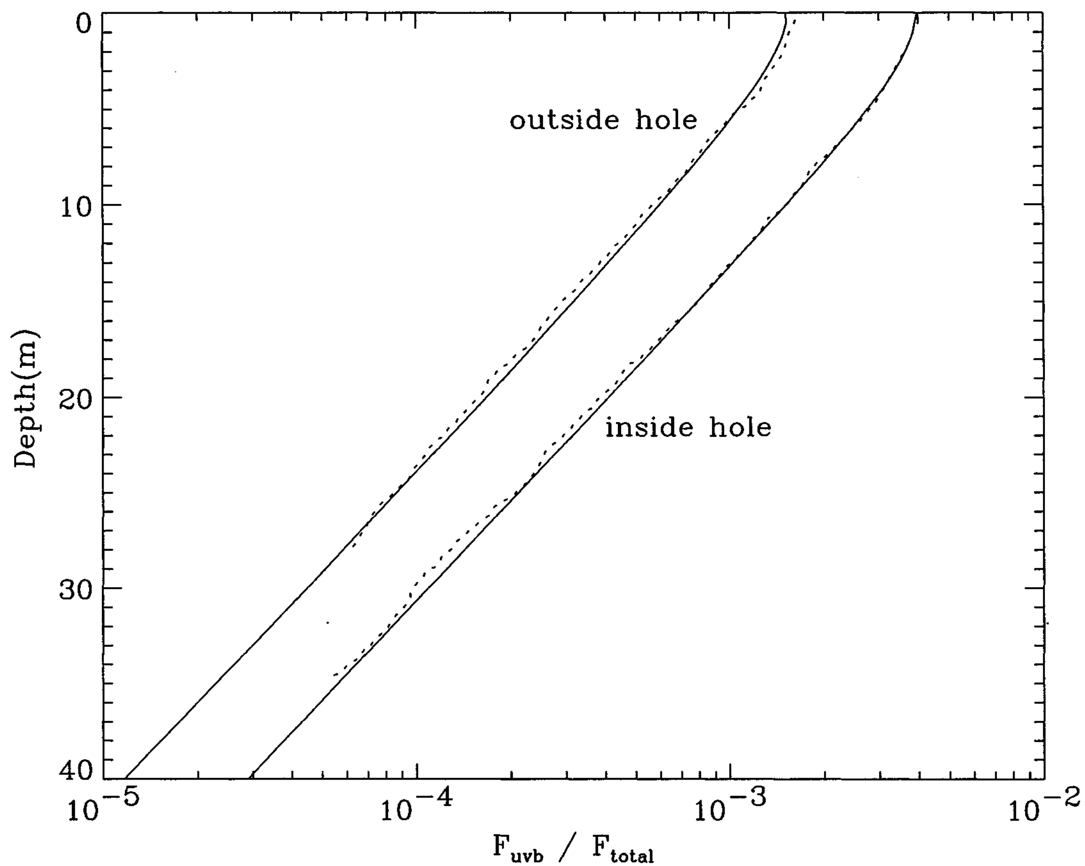

Figure 8: Comparison between model computations (solid lines) and measurements (dotted lines) of depth versus F_{UV-B}/F_{total}. Inside the ozone hole, the ozone abundance was 150 DU, the solar zenith angle was 56°, and the vertical distribution of chlorophyll concentration was 0.57 mg· m^{-3} from the surface to 20 m depth, 0.47 mg· m^{-3} below 20 m. Outside the ozone hole, the ozone abundance was 350 DU, the solar zenith angle was 57°, and the vertical distribution of chlorophyll concentration was 1.9 mg·m^{-3} from the surface to 10 m depth, 1.6 mg·m^{-3} from 10 to 20 m, and 1.5 mg· m^{-3} below 2 m.

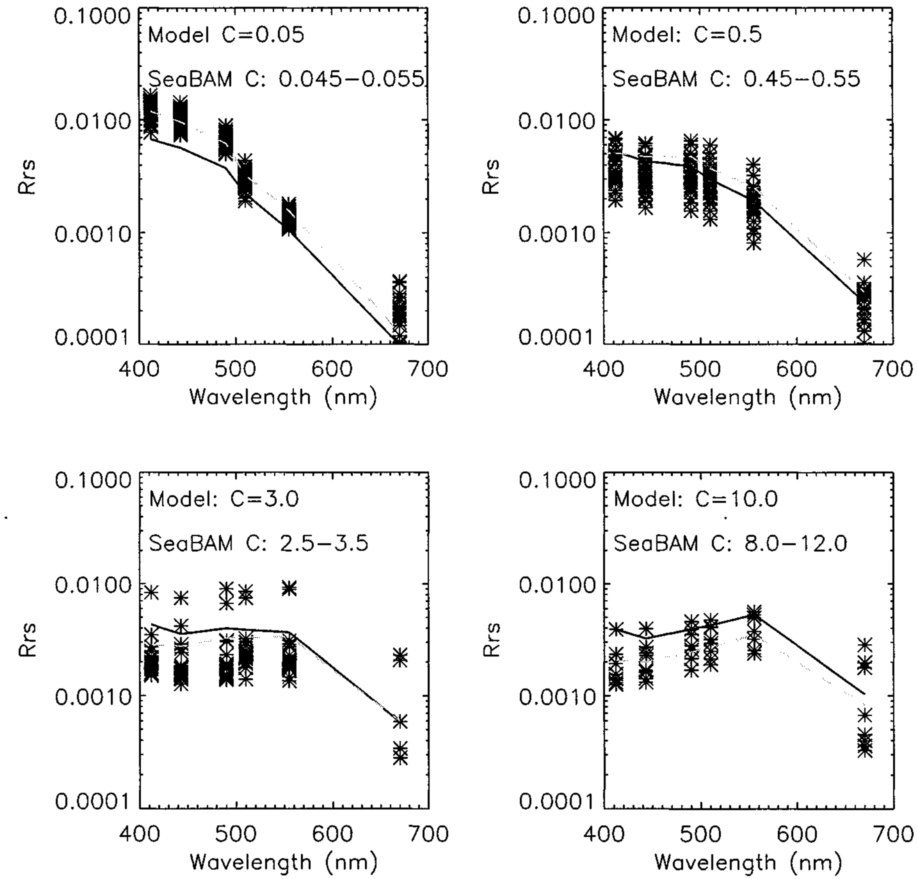

Figure 9: Comparisons between R_{rs} values computed from a radiative transfer model for the coupled atmosphere-ocean system and R_{rs} values from the SeaBAM data base for similar chlorophyll concentrations. Solid lines and dashed lines are the computed R_{rs} values based on the "old" Morel bio-optical model and the "new" modified Morel model, respectively. The stars represent the measured R_{rs} values provided in the SeaBAM data base.

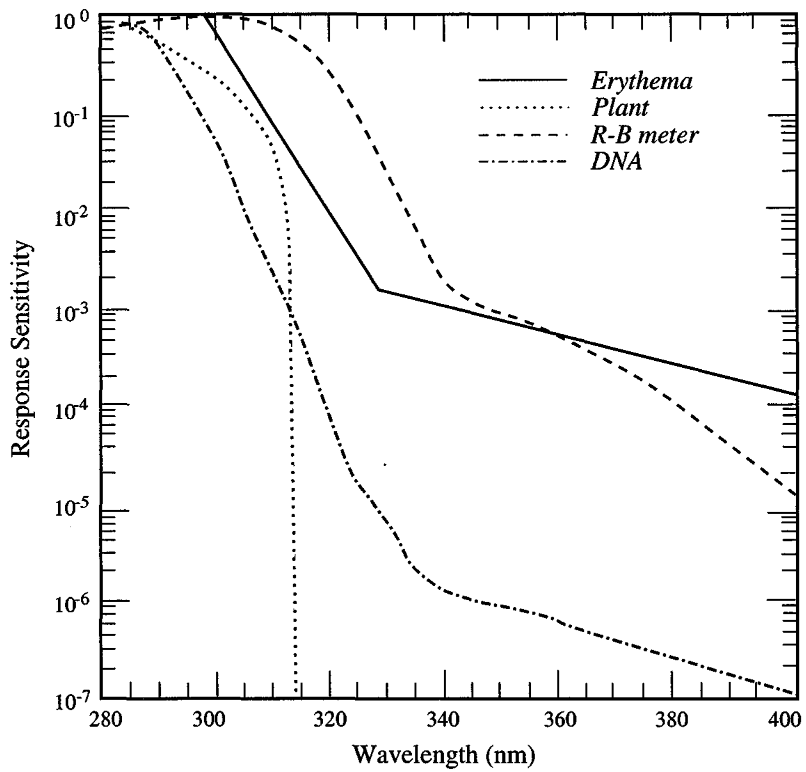

Figure 10: Action spectra for various biological responses. R-B meter stands for a measuring device, known as the *Robertson-Berger* meter, that was designed to mimic the sunburning response of Caucasian skin.

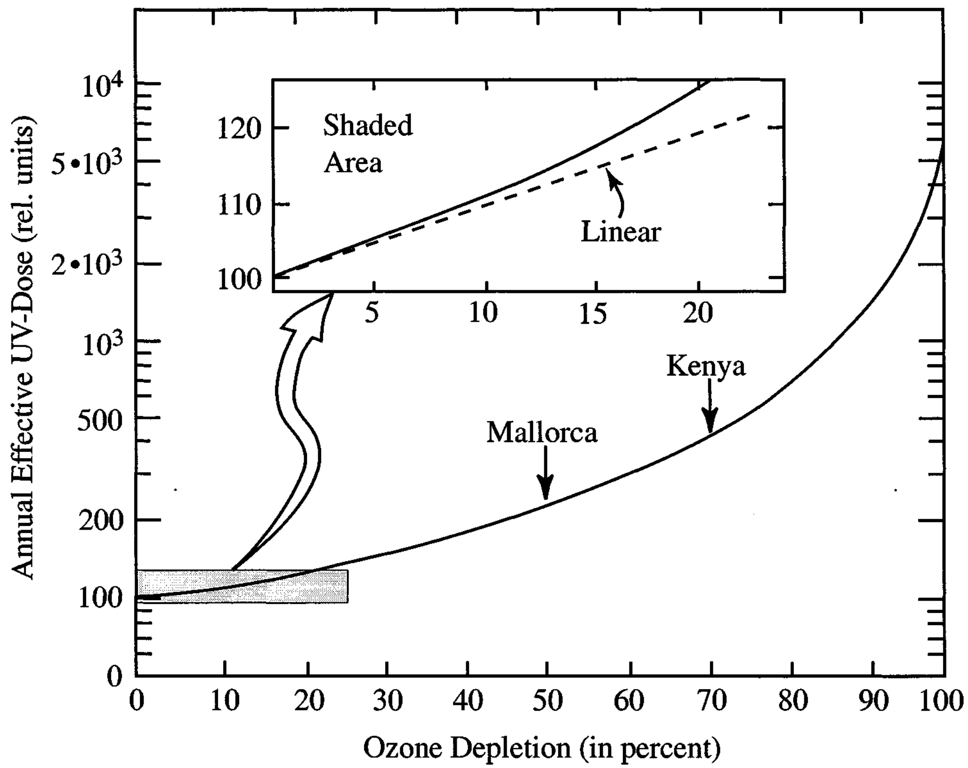

Figure 11: The annual effective UV dose at 60° N as a function of the ozone depletion (logarithmic scale). The annual UV dose, with normal ozone conditions throughout the year, is set to 100. The inset exhibits the dotted area with the dose axis enlarged and given a linear scale. The annual UV dose for latitude of 40° N (Mediterranean countries, California) and countries along the Equator, with normal ozone conditions, are indicated by Mollorca and Kenya, respectively.

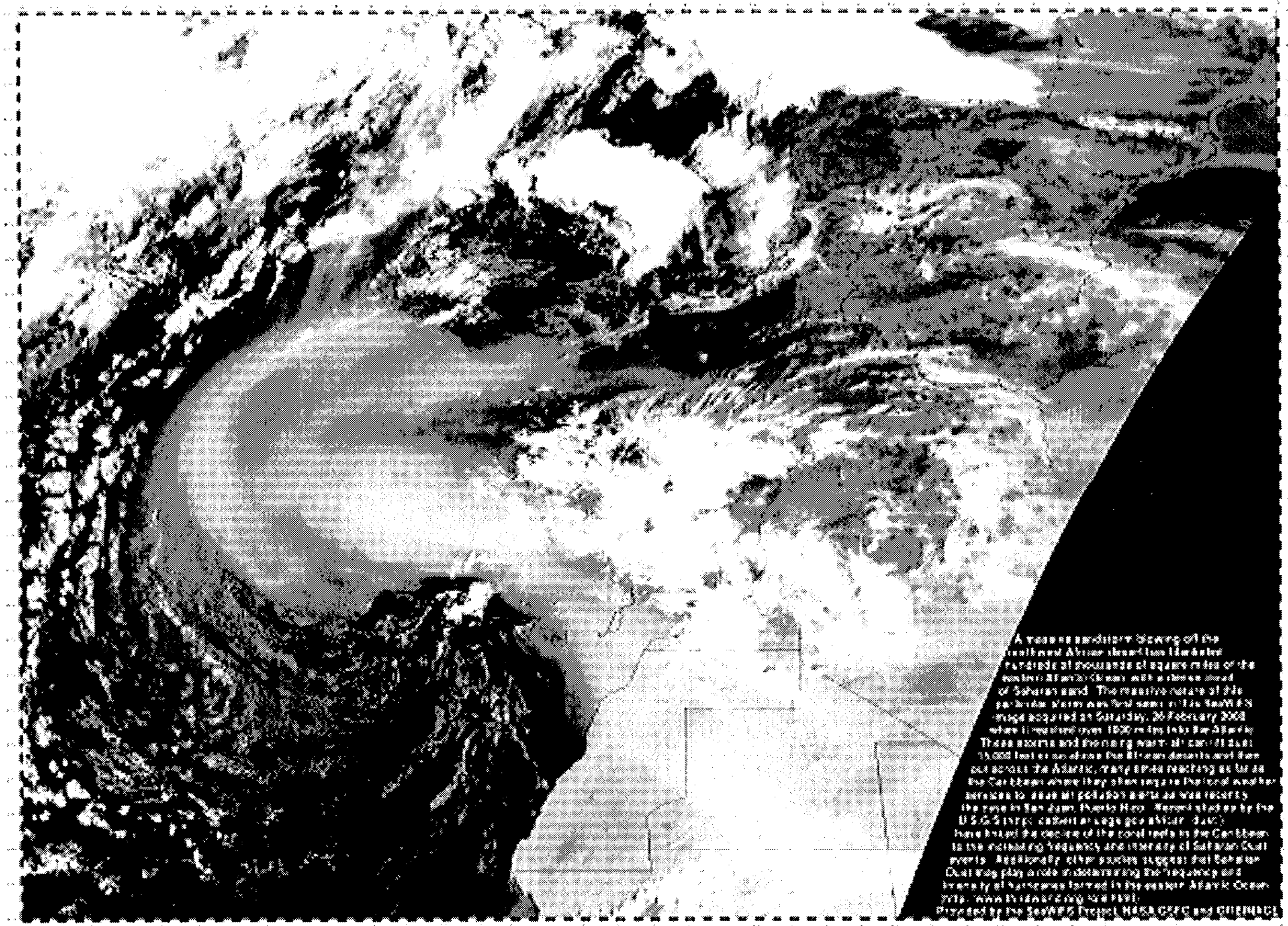

Figure 12: SeaWIFS image over Sharan Dust Blowing off African Coast.

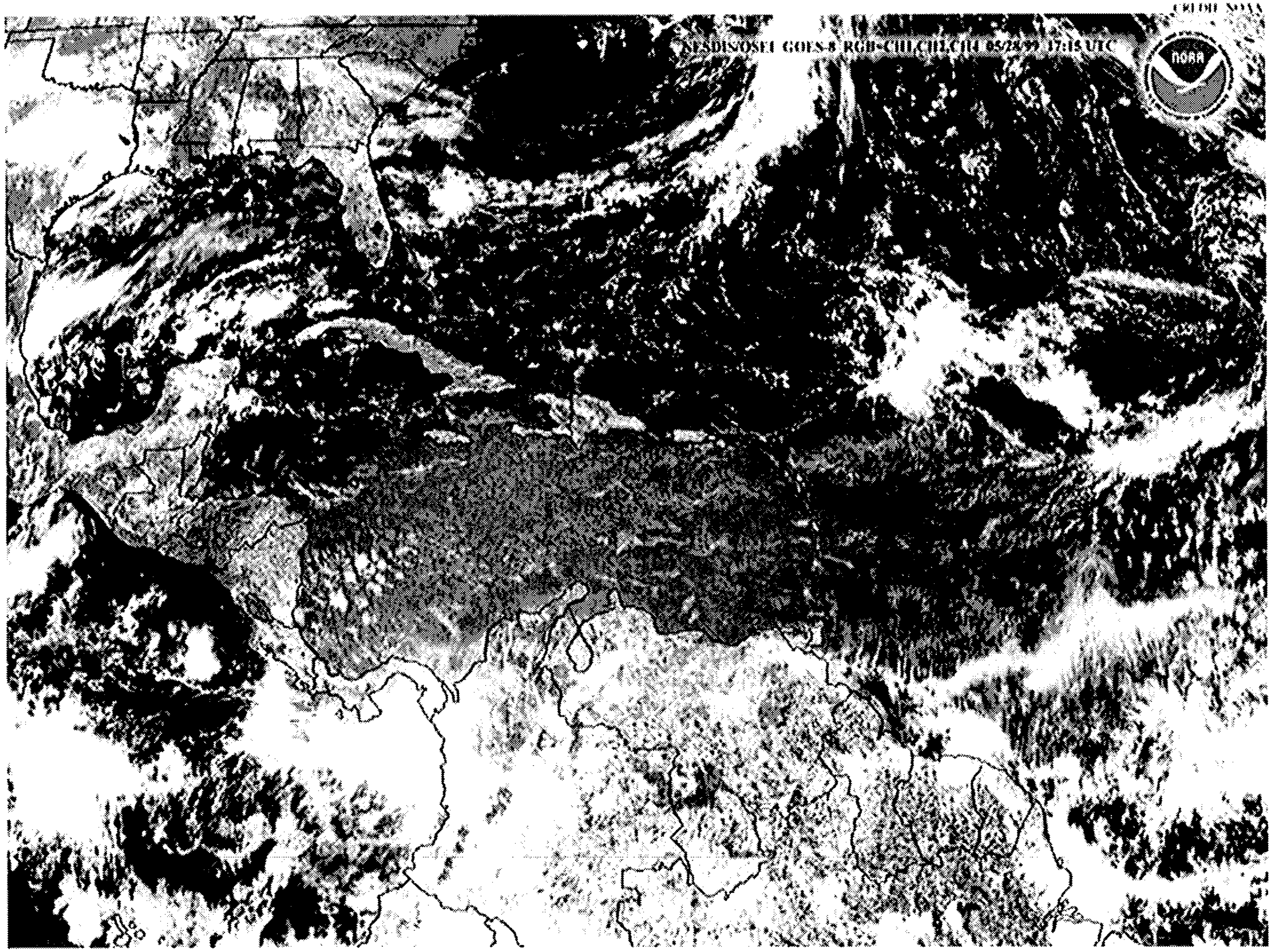

Figure 13: SeaWIFS image over the Carribean.

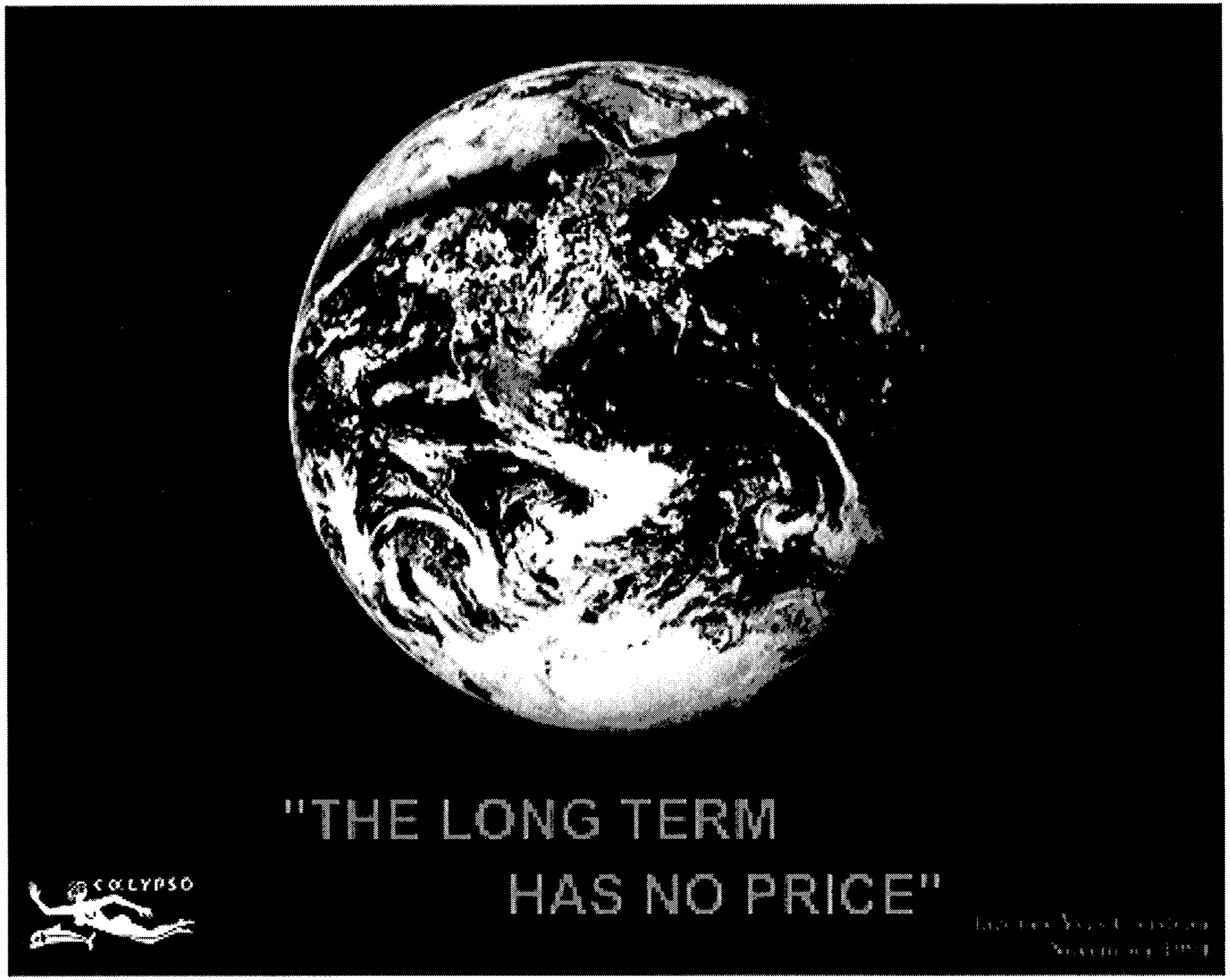

Figure 14: The Earth from Space.

The Two-Stream Approximation: Isotropic Scattering (0)

We need to solve the following set of coupled, linear differential equations:

$$\begin{aligned}
\mu_i \frac{dI^+(\tau,\mu_i)}{d\tau} &= I^+(\tau,\mu_i) - \frac{a}{2}\sum_{j=1}^{N} w_j p(\mu_j,\mu_i) I^+(\tau,\mu_j) \\
&- \frac{a}{2}\sum_{j=1}^{N} w_j p(-\mu_j,\mu_i) I^-(\tau,\mu_j) - Q^+(\tau,\mu_i) \qquad (1) \\
-\mu_i \frac{dI^-(\tau,\mu_i)}{d\tau} &= I^-(\tau,\mu_i) - \frac{a}{2}\sum_{j=1}^{N} w_j p(\mu_j,-\mu_i) I^+(\tau,\mu_j) \\
&- \frac{a}{2}\sum_{j=1}^{N} w_j p(-\mu_j,-\mu_i) I^-(\tau,\mu_j) - Q^-(\tau,\mu_i). \qquad (2)
\end{aligned}$$

where

$$\begin{aligned}
Q^\pm(\tau,\mu_i) &= X_{0i}^\pm \; e^{-\tau/\mu_0} + (1-a)B[\tau(T(z)] \\
X_{0i}^\pm \equiv X_0(\pm\mu_i) &= \frac{a}{4\pi} F_0 p(-\mu_0, \pm\mu_i).
\end{aligned}$$

The Two-Stream Approximation: Isotropic Scattering (1)

Approximate Differential Equations

The radiative transfer equations for the half-range intensity fields are given by (ignoring the beam source for the moment)

$$\mu \frac{dI^{+}(\tau,\mu)}{d\tau} = I^{+}(\tau,\mu) - \frac{a}{2}\int_0^1 d\mu' I^{+}(\tau,\mu') - \frac{a}{2}\int_0^1 d\mu' I^{-}(\tau,\mu') - (1-a)B$$

$$-\mu \frac{dI^{-}(\tau,\mu)}{d\tau} = I^{-}(\tau,\mu) - \frac{a}{2}\int_0^1 d\mu' I^{+}(\tau,\mu') - \frac{a}{2}\int_0^1 d\mu' I^{-}(\tau,\mu') - (1-a)B.$$

Because the scattering is isotropic, the radiation field has **no** azimuthal dependence.

- In the two-stream approximation we replace the angularly-dependent quantities $I^{\pm}$ by their averages over each hemisphere, $I^{+}(\tau)$ and $I^{-}(\tau)$ in each hemisphere.

The Two-Stream Approximation: Isotropic Scattering (2)

- This leads to the following pair of coupled differential equations which are called:

The two-stream equations

$$\bar{\mu}^{+}\frac{dI^{+}(\tau)}{d\tau} = I^{+}(\tau) - \frac{a}{2}I^{+}(\tau) - \frac{a}{2}I^{-}(\tau) - (1-a)B \tag{3}$$

$$-\bar{\mu}^{-}\frac{dI^{-}(\tau)}{d\tau} = I^{-}(\tau) - \frac{a}{2}I^{+}(\tau) - \frac{a}{2}I^{-}(\tau) - (1-a)B. \tag{4}$$

- Here $\bar{\mu}^{\pm}$ is the cosine of the average polar angle $\bar{\theta}$ made by a beam, which generally differs in the two hemispheres.
- These linear, coupled, ordinary differential equations allow for analytic solutions by standard methods if the medium is homogeneous so that $a(\tau) = a =$ constant.

The Two-Stream Approximation: Isotropic Scattering (3)

Note that the two-stream approximation:

- Will be most accurate when the radiation field is nearly isotropic: deep inside the medium, far away from any boundary, or from sources or sinks of radiation. However, often it is accurate even at the boundaries themselves.
- Can teach us about radiative transfer in optically-thin as well as optically-thick conditions, and for both scattering and emission-dominated problems.

The approximate two-stream expressions for the source function, the flux and the heating rate are

$$\begin{aligned} S(\tau) &= \frac{a}{2}\int_0^1 d\mu[I^+(\tau,\mu) + I^-(\tau,\mu)] + (1-a)B \\ &\approx \frac{a}{2}\left[I^+(\tau) + I^-(\tau)\right] + (1-a)B \end{aligned} \quad (5)$$

$$\begin{aligned} F(\tau) &= 2\pi\int_0^1 d\mu\mu[I^+(\tau,\mu) - I^-(\tau,\mu)] \\ &\approx 2\pi\left[\bar{\mu}^+ I^+(\tau) - \bar{\mu}^- I^-(\tau)\right] \end{aligned} \quad (6)$$

$$\mathcal{H}(\tau) = -\frac{\partial F}{\partial z} \approx 2\pi\alpha \left[I^{+}(\tau) + I^{-}(\tau)\right] - 4\pi\alpha B. \tag{7}$$

The Mean Inclination: Possible Choices for $\bar{\mu}$ (1)

- We could define $\bar{\mu}^{\pm}$ formally as the intensity-weighted angular means:

$$\bar{\mu}^{\pm} = \langle \mu \rangle^{\pm} \equiv \frac{2\pi \int_0^1 d\mu \mu I^{\pm}(\tau, \mu)}{2\pi \int_0^1 d\mu I^{\pm}(\tau, \mu)} = \frac{F^{\pm}}{2\pi I^{\pm}}$$

- Since we do not know the intensity distribution **a priori** this definition is of little use, but it demonstrates that $\bar{\mu}$ will vary with optical depth and take on a different value in the two hemispheres.
- Hence picking the same constant value for this quantity in both hemispheres ($\bar{\mu} = \bar{\mu}^{+} = \bar{\mu}^{-} =$ constant) is clearly an approximation.
- If the intensity field were strictly hemispherically-isotropic, this formula yields $\bar{\mu} = 1/2$ for all depths and for both hemispheres (same as for one-point Gaussian quadrature, see Chapter 8).
- If the intensity distribution were approximately linear in μ, say $I(\mu) \approx C\mu$, where C is a constant, then $\bar{\mu} = 2/3$.

Light and Life Laboratory STEVENS Institute of Technology

The Mean Inclination: Possible Choices for $\bar{\mu}$ (2)

- Alternatively, we could use the root-mean-square value:

$$\bar{\mu} \equiv \mu_{rms} = \sqrt{\langle \mu^2 \rangle} = \sqrt{\frac{\int_0^1 d\mu \mu^2 I(\tau, \mu)}{\int_0^1 d\mu I(\tau, \mu)}}.$$

- If the radiation field were isotropic this definition would yield $\bar{\mu} = 1/\sqrt{3}$. This is identical to the value obtained from a two-point Gaussian quadrature for the complete range of $u = \cos\theta$ $(-1 \leq u \leq 1)$.
- A linear variation of the radiation field would yield $\bar{\mu} = 1/\sqrt{2} = 0.71$.
- Thus, these possible choices yield $\bar{\mu}$-values ranging from 0.5 to 0.71. There is really no certain way to decide categorically and *a priori* which choice is optimal, or if there is another definition that would be even better.
- We have to pick the optimal $\bar{\mu}$-value on **a trial-and-error basis** for each type of problem. We now assume a single value for $\bar{\mu}$ but leave its value undetermined to remind us that it represents some sort of average over a hemisphere.

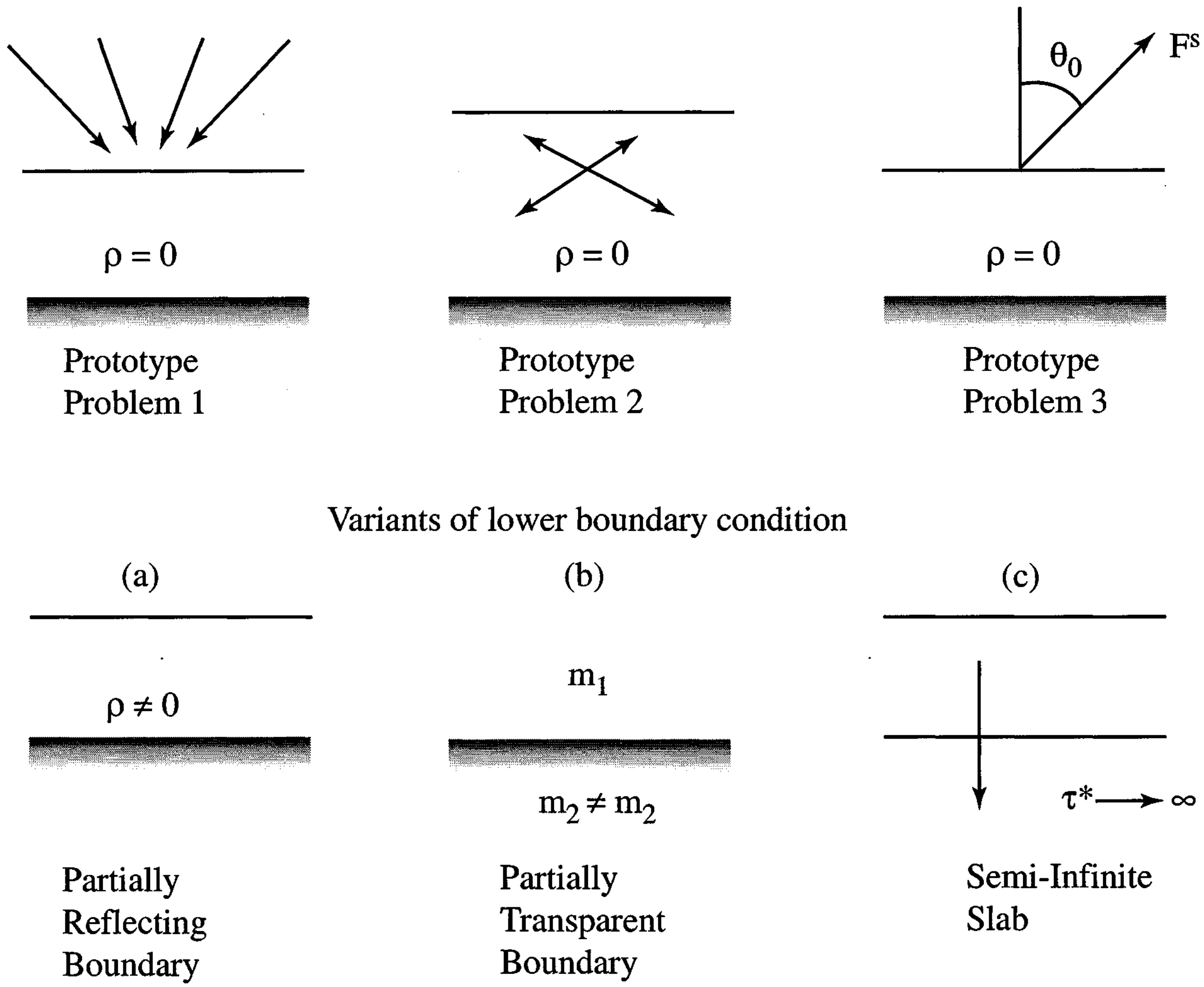

Figure 1: Illustration of Prototype Problems in radiative transfer.

Prototype Problem 1 (1)

We ignore the thermal emission term.

- By first adding eqns. 3 and 4 and then subtracting eqns. 4 from 3 we obtain:

$$\bar{\mu}\frac{d(I^+ - I^-)}{d\tau} = (1-a)(I^+ + I^-) \tag{8}$$

$$\bar{\mu}\frac{d(I^+ + I^-)}{d\tau} = (I^+ - I^-). \tag{9}$$

- Differentiating eqn. 9 with respect to τ, and substituting for $d(I^+ - I^-)/d\tau$ from eqn. 8, we find:

$$\frac{d^2(I^+ + I^-)}{d\tau^2} = \frac{(1-a)}{\bar{\mu}^2}(I^+ + I^-).$$

- This provides us with an equation involving only the **sum** of the intensities.

Prototype Problem 1 (2)

- Similarly, differentiating the first of the above equations, and substituting for $d(I^+ + I^-)/d\tau$ from the second equation, we find:

$$\frac{d^2(I^+ - I^-)}{d\tau^2} = \frac{(1-a)}{\bar{\mu}^2}(I^+ - I^-)$$

which involves only the **difference** of the intensities.

- We have the same differential equation to solve for both quantities. Calling the unknown, Y, we obtain a simple second-order **diffusion equation**

$$\frac{d^2Y}{d\tau^2} = \Gamma^2 Y \qquad \text{where } \Gamma \equiv \sqrt{1-a}/\bar{\mu}, \tag{10}$$

for which the general solution is a sum of positive and negative exponentials

$$Y = A'e^{\Gamma\tau} + B'e^{-\Gamma\tau}.$$

A' and B' are arbitrary constants to be determined.

Light and Life Laboratory STEVENS Institute of Technology

Prototype Problem 1 (3)

- Since the **sum** and **difference** of the two intensities are both expressed as sums of exponentials, each intensity component must be expressed in the same way:

$$I^+(\tau) = Ae^{\Gamma\tau} + Be^{-\Gamma\tau}; \qquad I^-(\tau) = Ce^{\Gamma\tau} + De^{-\Gamma\tau} \tag{11}$$

where A, B, C, and D are additional arbitrary constants.

- We now introduce boundary conditions at the top and the bottom of the medium. We begin with *Prototype Problem 1* for which:

$$I^-(\tau = 0) = \mathcal{I} = \text{ constant}; \qquad I^+(\tau^*) = 0. \tag{12}$$

- We choose this as our first example, as the two-stream solution to this problem has the simplest analytic form of the three considered.

Prototype Problem 1 (5)

- Eqns. 11 display four constants of integration, but the two boundary conditions, eqns. 12, and the fact that the differential equation is of degree two, suggest that there are only two independent constants.
- To obtain the two necessary relationships between A, B, C, and D, we substitute eqns. 11 into eqns. 3–4. We find that:

$$\frac{C}{A} = \frac{B}{D} = \frac{a}{2-a+2\bar{\mu}\Gamma} = \frac{1-\bar{\mu}\Gamma}{1+\bar{\mu}\Gamma} = \frac{1-\sqrt{1-a}}{1+\sqrt{1-a}} \equiv \rho_\infty. \tag{13}$$

- An explanation of the physical meaning of ρ_∞ is provided in Example 7.2.
- We now substitute into the general solutions, eqns. 11, to obtain:

$$I^+(\tau) = Ae^{\Gamma\tau} + \rho_\infty De^{-\Gamma\tau} \tag{14}$$
$$I^-(\tau) = \rho_\infty Ae^{\Gamma\tau} + De^{-\Gamma\tau}. \tag{15}$$

Prototype Problem 1 (6)

- We now apply the boundary conditions (eqns. 12) which yield:

$$I^-(\tau = 0) = \rho_\infty A + D = \mathcal{I} \quad ; \quad I^+(\tau = \tau^*) = Ae^{\Gamma\tau^*} + \rho_\infty De^{-\Gamma\tau^*} = 0.$$

- Solving for A and D we find:

$$A = \frac{-\rho_\infty \mathcal{I} e^{-\Gamma\tau^*}}{e^{\Gamma\tau^*} - \rho_\infty^2 e^{-\Gamma\tau^*}} \quad ; \quad D = \frac{\mathcal{I} e^{\Gamma\tau^*}}{e^{\Gamma\tau^*} - \rho_\infty^2 e^{-\Gamma\tau^*}}.$$

- The solutions are:

$$I^+(\tau) = \frac{\mathcal{I}\rho_\infty}{\mathcal{D}}\left[e^{\Gamma(\tau^*-\tau)} - e^{-\Gamma(\tau^*-\tau)}\right] \tag{16}$$

$$I^-(\tau) = \frac{\mathcal{I}}{\mathcal{D}}\left[e^{\Gamma(\tau^*-\tau)} - \rho_\infty^2 e^{-\Gamma(\tau^*-\tau)}\right] \tag{17}$$

where the denominator is

$$\mathcal{D} \equiv e^{\Gamma\tau^*} - \rho_\infty^2 e^{-\Gamma\tau^*}. \tag{18}$$

Prototype Problem 1 (7)

- The solutions for the source function, flux and heating rate follow from eqns. 5–7:

$$S(\tau) = \frac{a\mathcal{I}}{2\mathcal{D}}(1+\rho_\infty)\left[e^{\Gamma(\tau^*-\tau)} - \rho_\infty e^{-\Gamma(\tau^*-\tau)}\right] \tag{19}$$

$$F(\tau) = -2\bar{\mu}\frac{\pi\mathcal{I}}{\mathcal{D}}(1-\rho_\infty)\left[e^{\Gamma(\tau^*-\tau)} + \rho_\infty e^{-\Gamma(\tau^*-\tau)}\right] \tag{20}$$

$$\mathcal{H}(\tau) = \frac{2\pi\alpha\mathcal{I}}{\mathcal{D}}(1+\rho_\infty)[e^{\Gamma(\tau^*-\tau)} - \rho_\infty e^{-\Gamma(\tau^*-\tau)}]. \tag{21}$$

- Note that eqn. 6 yields $F^-(0) = 2\pi\bar{\mu}I^-(0) = 2\pi\bar{\mu}\mathcal{I}$ for the incoming flux at the top of the slab.

- We might be tempted to set $\bar{\mu} = 0.5$ so that this expression would yield the exact value, $\pi\mathcal{I}$. However, to remain consistent with the two-stream approximation, it is important to use the approximate expression, eqn. 6.

Prototype Problem 1 (8)

- The flux reflectance, flux transmittance, and absorptance become:

$$\rho(-2\pi, 2\pi) = \frac{2\pi\bar{\mu}I^+(0)}{2\pi\bar{\mu}\mathcal{I}} = \frac{\rho_\infty}{\mathcal{D}}[e^{\Gamma\tau^*} - e^{-\Gamma\tau^*}] \tag{22}$$

$$\mathcal{T}(-2\pi, -2\pi) = 2\pi\bar{\mu}\frac{I^-(\tau^*)}{2\pi\bar{\mu}\mathcal{I}} = \frac{1-\rho_\infty^2}{\mathcal{D}} \tag{23}$$

$$\begin{aligned} \alpha(-2\pi) &= 1 - \rho(-2\pi, 2\pi) - \mathcal{T}(-2\pi, -2\pi) \\ &= \frac{(1-\rho_\infty)}{\mathcal{D}}\left[e^{\Gamma\tau^*} + \rho_\infty e^{-\Gamma\tau^*} - 1 - \rho_\infty\right]. \end{aligned} \tag{24}$$

- Note: the flux transmittance includes the 'beam' transmittance:

$$\mathcal{T}_b(-2\pi, -2\pi) = \frac{\int_0^1 d\mu\mu\mathcal{I}e^{-\tau^*/\mu}}{\int_0^1 d\mu\mu\mathcal{I}} = 2E_3(\tau^*).$$

Light and Life Laboratory STEVENS Institute of Technology

Prototype Problem 1 (9)

- Thus, the diffuse flux transmittance is:

$$\mathcal{T}_d(-2\pi, -2\pi) = \mathcal{T}(-2\pi, -2\pi) - \mathcal{T}_b(-2\pi, -2\pi) = \frac{1 - \rho_\infty^2}{\mathcal{D}} - 2E_3(\tau^*). \qquad (25)$$

Example: Angular Distribution of the Radiation Field (1)

- To find the intensity $I^{\pm}(\tau,\mu)$ in the two-stream approximation, it is necessary to integrate the (approximate) source function.
- This method yields a closed-form solution for the angular dependence of the intensity, and may provide sufficient accuracy for some problems.
- We proceed by considering the expressions for the upward and downward intensity:

$$\begin{aligned} I^{+}(\tau,\mu) &= \int_{\tau}^{\tau^*} \frac{d\tau'}{\mu} S(\tau') e^{-(\tau'-\tau)/\mu} \\ I^{-}(\tau,\mu) &= \int_{0}^{\tau} \frac{d\tau'}{\mu} S(\tau') e^{-(\tau-\tau')/\mu} + \mathcal{I} e^{-\tau/\mu}. \end{aligned} \tag{26}$$

Light and Life Laboratory STEVENS Institute of Technology

Example: Angular Distribution of the Radiation Field (2)

• Inserting the approximate two-stream source function:

$$S(\tau) = \frac{a\mathcal{I}}{2\mathcal{D}}(1+\rho_\infty)\left[e^{\Gamma(\tau^*-\tau)} - \rho_\infty e^{-\Gamma(\tau^*-\tau)}\right]$$

and performing the integration, we find:

$$\begin{aligned} I^+(\tau,\mu) &= \frac{\mathcal{I}\rho_\infty}{\mathcal{D}}\{C^+(\mu)e^{\Gamma(\tau^*-\tau)} - C^-(\mu)e^{-\Gamma(\tau^*-\tau)} \\ &\quad + [C^-(\mu) - C^+(\mu)]e^{-(\tau^*-\tau)/\mu}\} \end{aligned} \tag{27}$$

$$\begin{aligned} I^-(\tau,\mu) &= \frac{\mathcal{I}}{\mathcal{D}}\{C^-(\mu)e^{\Gamma(\tau^*-\tau)} - C^+(\mu)\rho_\infty^2 e^{-\Gamma(\tau^*-\tau)} + [1-C^-(\mu)]e^{\Gamma\tau^*-\tau/\mu} \\ &\quad - \rho_\infty^2[1-C^+(\mu)]e^{-\Gamma\tau^*-\tau/\mu}\} \end{aligned} \tag{28}$$

where $C^{\pm}(\mu) \equiv (1 \pm \Gamma\bar{\mu})/(1 \pm \Gamma\mu)$.

Light and Life Laboratory STEVENS Institute of Technology

Prototype Problem 3: Beam Incidence (1)

- We now consider the most important scattering problem in planetary atmospheres – that of a collimated solar beam of flux F^s, incident from above on a planetary atmosphere.
- We simplify to an isotropically-scattering, homogeneous atmosphere and, as usual, assume a black lower boundary. (Both these restrictions will be removed later.)

Setting the angle of incidence to be $\theta_0 = \cos^{-1}\mu_0$, we find that the appropriate two-stream equations are:

$$\bar{\mu}\frac{dI_d^+}{d\tau} = I_d^+ - \frac{a}{2}(I_d^+ + I_d^-) - \frac{a}{4\pi}F^s e^{-\tau/\mu_0} \tag{29}$$

$$-\bar{\mu}\frac{dI_d^-}{d\tau} = I_d^- - \frac{a}{2}(I_d^+ + I_d^-) - \frac{a}{4\pi}F^s e^{-\tau/\mu_0} \tag{30}$$

where I_d^+ and I_d^- are the diffuse intensities.

Prototype Problem 3: Beam Incidence (2)

As before, we take the sum and difference of the above equations:

$$\bar{\mu}\frac{d(I_d^+ - I_d^-)}{d\tau} = (1-a)(I_d^+ + I_d^-) - \frac{a}{2\pi}F^s e^{-\tau/\mu_0} \quad (31)$$

$$\bar{\mu}\frac{d(I_d^+ + I_d^-)}{d\tau} = (I_d^+ - I_d^-). \quad (32)$$

- Differentiating eqn. 32 and substituting into eqn. 31, we find:

$$\bar{\mu}^2\frac{d^2(I_d^+ + I_d^-)}{d\tau^2} = (1-a)(I_d^+ + I_d^-) - \frac{a}{2\pi}F^s e^{-\tau/\mu_0}.$$

- Similarly, if we differentiate eqn. 31 and substitute into eqn. 32 we get:

$$\bar{\mu}^2\frac{d^2(I_d^+ - I_d^-)}{d\tau^2} = (1-a)(I_d^+ - I_d^-) + \frac{a\bar{\mu}}{2\pi\mu_0}F^s e^{-\tau/\mu_0}.$$

Light and Life Laboratory STEVENS Institute of Technology

Prototype Problem 3: Beam Incidence (3)

- We may use the same solution method used earlier for *Prototype Problem 2*. As was shown previously, the homogeneous solution can be written as follows:

$$I_d^+ = Ae^{\Gamma\tau} + \rho_\infty De^{-\Gamma\tau}; \qquad I_d^- = \rho_\infty Ae^{\Gamma\tau} + De^{-\Gamma\tau}$$

where Γ and ρ_∞ have their usual meanings.

- We guess that the particular solution is proportional to $e^{-\tau/\mu_0}$. Thus, we set:

$$I_d^+ = Ae^{\Gamma\tau} + \rho_\infty De^{-\Gamma\tau} + Z^+ e^{-\tau/\mu_0}$$

$$I_d^- = \rho_\infty Ae^{\Gamma\tau} + De^{-\Gamma\tau} + Z^- e^{-\tau/\mu_0}$$

where Z^+ and Z^- are constants to be determined.

- Substituting into eqns. 29–30, we find:

$$Z^+ + Z^- = -\frac{aF^s\mu_0^2}{2\pi\bar{\mu}^2(1-\Gamma^2\mu_0^2)}; \quad Z^+ - Z^- = \frac{aF^s\mu_0\bar{\mu}}{2\pi\bar{\mu}^2(1-\Gamma^2\mu_0^2)}. \qquad (33)$$

Prototype Problem 3: Beam Incidence (4)

- The above two equations may be solved for Z^+ and Z^- separately:

$$Z^+ = \frac{aF^s\mu_0(\bar{\mu} - \mu_0)}{4\pi\bar{\mu}^2(1 - \Gamma^2\mu_0^2)}; \qquad Z^- = -\frac{aF^s\mu_0(\mu_0 + \bar{\mu})}{4\pi\bar{\mu}^2(1 - \Gamma^2\mu_0^2)}. \tag{34}$$

- We apply boundary conditions for the diffuse intensity: $I_d^-(\tau = 0) = 0$ and $I_d^+(\tau^*) = 0$. From these two conditions, we obtain two simultaneous equations for A and D. After some manipulation we find:

$$A = -\frac{aF^s\mu_0}{4\pi\bar{\mu}^2(1 - \Gamma^2\mu_0^2)\mathcal{D}}\left[\rho_\infty(\bar{\mu} + \mu_0)e^{-\Gamma\tau^*} + (\bar{\mu} - \mu_0)e^{-\tau^*/\mu_0}\right]$$

$$D = \frac{aF^s\mu_0}{4\pi\bar{\mu}^2(1 - \Gamma^2\mu_0^2)\mathcal{D}}\left[(\bar{\mu} + \mu_0)e^{\Gamma\tau^*} + \rho_\infty(\bar{\mu} - \mu_0)e^{-\tau^*/\mu_0}\right]$$

where $\mathcal{D}$ is defined in eqn. 18.

Prototype Problem 3: Beam Incidence (5)

- We may now solve for the source function, flux etc. For example, the source function is:

$$S(\tau) = \frac{a}{2}(I_d^+ + I_d^-) + \frac{aF^s}{4\pi}e^{-\tau/\mu_0}. \tag{35}$$

- Rather than display the rather complicated solution for a finite medium, we will consider the simpler situation of a semi-infinite medium. With the condition on the boundedness of the solution $S(\tau)e^{\tau} \rightarrow 0$, the positive exponentials must be discarded, so that $A = 0$. The constant D reduces to:

$$D = \frac{aF^s\mu_0(\bar{\mu} + \mu_0)}{4\pi\bar{\mu}^2(1 - \Gamma^2\mu_0^2)}.$$

Prototype Problem 3: Beam Incidence (6)

- The diffuse intensities are:

$$
\begin{aligned}
I_d^+(\tau) &= \rho_\infty D e^{-\Gamma\tau} + Z^+ e^{-\tau/\mu_0} \\
&= \frac{aF^s\mu_0}{4\pi\bar{\mu}^2(1-\Gamma^2\mu_0^2)}[\rho_\infty(\bar{\mu}+\mu_0)e^{-\Gamma\tau} + (\bar{\mu}-\mu_0)e^{-\tau/\bar{\mu}}] \qquad (36)
\end{aligned}
$$

$$
\begin{aligned}
I_d^-(\tau) &= D e^{-\Gamma\tau} + Z^- e^{-\Gamma/\mu_0} \\
&= \frac{aF^s\mu_0}{4\pi\bar{\mu}^2(1-\Gamma^2\mu_0^2)}[(\bar{\mu}+\mu_0)e^{-\Gamma\tau} - (\bar{\mu}+\mu_0)e^{-\tau/\mu_0}] \qquad (37)
\end{aligned}
$$

and the source function becomes (eqn. 35):

$$
\begin{aligned}
S(\tau) &= \frac{aF^s}{4\pi}\{\frac{a\mu_0}{\bar{\mu}^2(1-\Gamma^2\mu_0^2)}[\frac{1}{2}(\bar{\mu}+\mu_0)(1+\rho_\infty)e^{-\Gamma\tau} \\
&\quad - \mu_0 e^{-\tau/\mu_0}] + e^{-\tau/\mu_0}\}.
\end{aligned}
\qquad (38)
$$

Prototype Problem 3: Beam Incidence (7)

- We may ask: what happens if the denominator $(1-\Gamma^2\mu_0^2)$ is zero in the equations for $I_d^{\pm}$? This can occur if the sun is at a specific location in the sky.
- It turns out that this is a so-called *removable singularity*, that can be 'cured' by the application of *L'Hôspital's rule*, which leads to a new algebraic form that varies as $\tau \exp(-\tau/\mu_0)$.
- In computational work it is usually sufficient to use numerical 'dithering' by which μ_0 is changed slightly away from the 'singular value'. This artifice produces satisfactory results, and avoids the 'inconvenience' of having to deal with a special case involving a different solution.

Anisotropic Scattering: Two-Stream versus Eddington Approximations (1)

- Two-stream types of approximations are used primarily to compute fluxes and mean intensities in plane geometry.
- Flux and mean intensity depend only on the azimuthally-averaged radiation field. We are therefore interested in simple solutions to the azimuthally-averaged radiative transfer equation valid for anisotropic scattering:

$$u\frac{dI_d(\tau,u)}{d\tau} = I_d(\tau,u) - \frac{a}{2}\int_{-1}^{1} du' p(u',u) I_d(\tau,u') - S^*(\tau,u). \qquad (39)$$

- To obtain approximate solutions, we proceed by integrating eqn. 39 over each hemisphere to find two coupled, first-order differential equations for hemispherically-averaged upward and downward intensity 'streams'.
- For now, we ignore thermal emission.

Light and Life Laboratory STEVENS Institute of Technology

Anisotropic Scattering: Two-Stream versus Eddington Approximations (2)

- This leads to the usual **two-stream approximation.** We can obtain a similar result by replacing the integral in eqn. 39 by a two-term quadrature.
- We may alternatively proceed by approximating the angular dependence of the intensity by a polynomial in u. By choosing a linear polynomial, $I(\tau, u) = I_0(\tau) + uI_1(\tau)$, and taking angular moments of eqn. 39, we arrive at two coupled equations for the zeroth and first moments of the intensity, I_0 and I_1. This approach is usually referred to as the **Eddington approximation**.
- In the following, we examine both the Eddington and the two-stream approximation. We shall be particularly interested in exposing the similarities and differences between these two approaches.
- Assuming collimated incidence, $S^*(\tau, u) = (aF^s/4\pi)p(-\mu_0, u)e^{-\tau/\mu_0}$, we approximate the angular dependence of the intensity as $I(\tau, u) \approx [I_0(\tau) + uI_1(\tau)]$, which upon substitution into eqn. 39 yields:

Light and Life Laboratory STEVENS Institute of Technology

Anisotropic Scattering: Two-Stream versus Eddington Approximations (3)

$$u\frac{d(I_0 + uI_1)}{d\tau} = (I_0+uI_1) - \frac{a}{2}\int_{-1}^{1} du' p(u',u)(I_0+u'I_1) - \frac{aF^s}{4\pi}p(-\mu_0,u)e^{-\tau/\mu_0}. \quad (40)$$

- We expand the phase function in Legendre polynomials as usual, and find that the azimuthally-averaged phase function is:

$$p(u',u) = \sum_{l=0}^{\infty}(2l+1)\chi_l P_l(u)P_l(u')$$

where the moments of the phase function are given by:

$$\chi_l = \frac{1}{2}\int_{-1}^{+1} du' p(u',u)P_l(u').$$

- In the TSA, we normally retain only two terms: (1) the zeroth moment which is unity because of the normalization of the phase function ($\chi_0 = 1$); and (2) the first moment which we refer to as the **asymmetry factor**, $g \equiv \chi_1$.

Light and Life Laboratory STEVENS Institute of Technology

Anisotropic Scattering: Two-Stream versus Eddington Approximations (4)

Then:

$$\frac{a}{2}\int_{-1}^{1} du' p(u',u)(I_0 + u'I_1) = a(I_0 + 3gu\langle u\rangle_2 I_1)$$

where the $\langle\ \rangle$ symbol denotes an angular average over the sphere:

$$\langle u\rangle_2 \equiv \frac{1}{2}\int_{-1}^{1} du u^2.$$

Since $p(-\mu_0, u) = 1 - 3gu\mu_0$, eqn. 40 becomes:

$$u\frac{d(I_0 + uI_1)}{d\tau} = I_0 + uI_1 - a(I_0 + 3gu\langle u\rangle_2 I_1) - \frac{aF^s}{4\pi}(1 - 3gu\mu_0)e^{-\tau/\mu_0}. \quad (41)$$

- We first integrate eqn. 41 over u (from -1 to 1). This yields the first equation below. We then multiply eqn. 41 by u, and integrate again, to obtain the second equation below.

Light and Life Laboratory STEVENS Institute of Technology

Anisotropic Scattering: Two-Stream versus Eddington Approximations (5)

- Thus, we are left with the following pair of coupled equations for the moments of intensity, I_0 and I_1:

$$\frac{dI_1}{d\tau} = \frac{1}{\langle u \rangle_2}(1-a)I_0 - \frac{aF^s}{4\pi\langle u \rangle_2}e^{-\tau/\mu_0} \tag{42}$$

$$\frac{dI_0}{d\tau} = (1 - 3ga\langle u \rangle_2)I_1 + \frac{3aF^s}{4\pi}g\mu_0 e^{-\tau/\mu_0}. \tag{43}$$

- Rather than solve these coupled equations immediately, we consider a slightly different approach.
- We start by writing eqn. 39 in terms of the half-range intensities:

$$\begin{aligned}\mu\frac{dI_d^+(\tau,\mu)}{d\tau} &= I_d^+(\tau,\mu) - \frac{a}{2}\int_0^1 d\mu' p(-\mu',\mu)I_d^-(\tau,\mu') \\ &\quad - \frac{a}{2}\int_0^1 d\mu' p(\mu',\mu)I_d^+(\tau,\mu') - \frac{aF^s}{4\pi}p(-\mu_0,\mu)e^{-\tau/\mu_0} \\ &\equiv I_d^+(\tau,\mu) - S^+(\tau,\mu) \end{aligned} \tag{44}$$

Anisotropic Scattering: Two-Stream versus Eddington Approximations (6)

$$
\begin{aligned}
-\mu\frac{dI_d^-(\tau,\mu)}{d\tau} &= I_d^-(\tau,\mu) - \frac{a}{2}\int_0^1 d\mu' p(-\mu',-\mu) I_d^-(\tau,\mu') \\
&\quad - \frac{a}{2}\int_0^1 d\mu' p(\mu',-\mu) I_d^+(\tau,\mu') - \frac{aF^s}{4\pi} p(-\mu_0,-\mu) e^{-\tau/\mu_0}. \\
&\equiv I_d^-(\tau,\mu) - S^-(\tau,\mu) \qquad (45)
\end{aligned}
$$

- The above equations are 'exact'.
- We proceed by integrating both equations over the hemisphere by applying the operator $\int_0^1 d\mu$.
- If the $I^{\pm}(\tau,\mu)$ are replaced by their averages over each hemisphere, $I^{\pm}(\tau)$, and the explicit appearance of μ is replaced by some average value $\bar{\mu}$, this leads to the following pair of coupled equations for $I^{\pm}$ (dropping the 'd' subscript):

Light and Life Laboratory STEVENS Institute of Technology

Anisotropic Scattering: Two-Stream versus Eddington Approximations (7)

$$\bar{\mu}\frac{dI^+}{d\tau} = I^+ - a(1-b)I^+ - abI^- - S^{*+} \tag{46}$$

$$-\bar{\mu}\frac{dI^-}{d\tau} = I^- - a(1-b)I^- - abI^+ - S^{*-} \tag{47}$$

where

$$\begin{aligned} S^{*+} &\equiv \frac{aF^s}{2\pi}b(\mu_0)e^{-\tau/\mu_0} \equiv X^+(\tau)e^{-\tau/\mu_0} \\ S^{*-} &\equiv \frac{aF^s}{2\pi}[1-b(\mu_0)]e^{-\tau/\mu_0} \equiv X^-(\tau)e^{-\tau/\mu_0}. \end{aligned} \tag{48}$$

Here

$$X^+(\tau) \equiv \frac{a}{2\pi}F^s b(\mu_0); \qquad X^-(\tau) \equiv \frac{a}{2\pi}F^s[1-b(\mu_0)]. \tag{49}$$

Anisotropic Scattering: Two-Stream versus Eddington Approximations (8)

- The **backscattering coefficients** are defined as:

$$b(\mu) \equiv \frac{1}{2}\int_0^1 d\mu' \, p(-\mu', \mu) = \frac{1}{2}\int_0^1 d\mu' \, p(\mu', -\mu) \tag{50}$$

$$b \equiv \int_0^1 d\mu \, b(\mu) = \frac{1}{2}\int_0^1 d\mu \int_0^1 d\mu' \, p(-\mu', \mu) = \frac{1}{2}\int_0^1 d\mu \int_0^1 d\mu' \, p(\mu', -\mu) \tag{51}$$

$$1 - b = \frac{1}{2}\int_0^1 d\mu \int_0^1 d\mu' \, p(\mu', \mu) = \frac{1}{2}\int_0^1 d\mu \int_0^1 d\mu' \, p(-\mu', -\mu). \tag{52}$$

- We have used the **Reciprocity Relations** satisfied by the phase function, $p(-\mu', \mu) = p(\mu', -\mu)$; $p(-\mu', -\mu) = p(\mu', \mu)$, as well as the normalization property.

Anisotropic Scattering: Two-Stream versus Eddington Approximations (9)

- Equations 46 and 47 are the two-stream equations for anisotropic scattering. In the limit of isotropic scattering, ($p = 1$ or $b = \frac{1}{2}$), they reduce to the equations considered in the previous section, as they should.
- We note that if we choose $\bar{\mu} = 1/\sqrt{3}$, then the backscattering coefficient and the asymmetry factor are related through $b = \frac{1}{2}(1 - g)$.
- We have derived two sets of differential equations (eqns. 42 and 43) and (eqns. 46 and 47), both of which are derived from similar assumptions. What is the relationship, if any, between them?
- To answer this question, we will attempt to bring eqns. 46 and 47 into a form similar to eqns. 42 and 43. We do so by using the change of variable

$$I^{\pm}(\tau) = I_0 \pm \bar{\mu} I_1$$

consistent with the Eddington approximation.

Anisotropic Scattering: Two-Stream versus Eddington Approximations (10)

- By first adding eqns. 46 and 47, and then subtracting 46 from 47, we find after some manipulation that eqns. 46 and 47 are equivalent to:

$$\frac{dI_1}{d\tau} = \frac{1-a}{\bar{\mu}^2} I_0 - \frac{a}{4\pi\bar{\mu}^2} F^s e^{-\tau/\mu_0}$$

$$\frac{dI_0}{d\tau} = (1 - a + 2ab) I_1 + \frac{a}{4\pi\bar{\mu}} F^s [1 - 2b(\mu_0)] e^{-\tau/\mu_0}.$$

- Since $1 - a + 2ab = 1 - a + a(1 - 3g\bar{\mu}^2) = 1 - 3ag\bar{\mu}^2$ and $1 - 2b(\mu_0) = 1 - (1 - 3g\bar{\mu}\mu_0) = 3g\bar{\mu}\mu_0$, these last two equations become:

$$\frac{dI_1}{d\tau} = \frac{1-a}{\bar{\mu}^2} I_0 - \frac{a}{4\pi\bar{\mu}^2} F^s e^{-\tau/\mu_0} \tag{53}$$

$$\frac{dI_0}{d\tau} = (1 - 3ga\bar{\mu}^2) I_1 + \frac{3a}{4\pi} g\mu_0 F^s e^{-\tau/\mu_0}. \tag{54}$$

Light and Life Laboratory STEVENS Institute of Technology

Anisotropic Scattering: Two-Stream versus Eddington Approximations (11)

- Comparing eqns. 42–43 and 53–54, we conclude that **the equations describing the Eddington and two-stream approximations are identical provided** $\langle u \rangle_2 = \bar{\mu}^2$.
- Thus, the choices $\langle u \rangle_2 = \frac{1}{3}$ and $\bar{\mu} = 1/\sqrt{3}$ make the governing equations for the two methods the same.
- Therefore any remaining difference between the two must stem from different boundary conditions.
- This is readily seen as follows: A homogeneous boundary condition for the downward diffuse intensity consistent with the two-stream approximation leads to the boundary condition:

$$I^{-}(0) = I_0 - \bar{\mu} I_1 = 0.$$

Anisotropic Scattering: Two-Stream versus Eddington Approximations (12)

- If, however, we require the downward diffuse **flux** to be zero at the upper boundary (common practice in the Eddington approximation), then we find:

$$I_0 - \frac{2}{3} I_1 = 0.$$

- The value $\bar{\mu} = 1/\sqrt{3}$ for the average cosine follows from applying full-range Gaussian quadrature (see Chapter 8) while a half-range Gaussian quadrature would lead to $\bar{\mu} = \frac{1}{2}$.

Two-Stream Solutions for Anisotropic Scattering (1)

Focussing first on the homogeneous solution, we add and subtract eqns. 46 and 47 to obtain:

$$\frac{d(I_d^+ + I_d^-)}{d\tau} = -(\alpha - \beta)(I_d^+ - I_d^-) \tag{55}$$

$$\frac{d(I_d^+ - I_d^-)}{d\tau} = -(\alpha + \beta)(I_d^+ + I_d^-) \tag{56}$$

where we have defined $\alpha \equiv -[1 - a(1-b)]/\bar{\mu}$ and $\beta \equiv ab/\bar{\mu}$.

- By differentiating one equation and substituting into the second, we obtain the following uncoupled equations to solve:

$$\frac{d^2(I_d^+ + I_d^-)}{d\tau^2} = \Gamma^2(I_d^+ + I_d^-); \qquad \frac{d^2(I_d^+ - I_d^-)}{d\tau^2} = \Gamma^2(I_d^+ - I_d^-) \tag{57}$$

where

$$\Gamma = \sqrt{(\alpha - \beta)(\alpha + \beta)} = (1/\bar{\mu})\sqrt{(1-a)(1-a+2ab)}. \tag{58}$$

Light and Life Laboratory STEVENS Institute of Technology

Two-Stream Solutions for Anisotropic Scattering (2)

As in the case of isotropic scattering, the homogeneous solutions are:

$$I_d^+(\tau) = Ae^{\Gamma\tau} + Be^{-\Gamma\tau} = Ae^{\Gamma\tau} + \rho_\infty De^{-\Gamma\tau} \tag{59}$$

$$I_d^-(\tau) = Ce^{\Gamma\tau} + De^{-\Gamma\tau} = \rho_\infty Ae^{\Gamma\tau} + De^{-\Gamma\tau}. \tag{60}$$

- The coefficients A, B, C, and D are NOT all independent as pointed out previously. The relation between them is found by substituting eqns. 59 and 60 into eqns. 46 and 47, yielding:

$$\frac{C}{A} = \frac{B}{D} = \frac{\sqrt{1-a+2ab} - \sqrt{1-a}}{\sqrt{1-a+2ab} + \sqrt{1-a}} \equiv \rho_\infty.$$

- Equations. 46 and 47 suggest seeking a particular solution of the form:

$$I_d^\pm = Z^\pm e^{-\tau/\mu_0}. \tag{61}$$

Two-Stream Solutions for Anisotropic Scattering (3)

Substitution of eqn. 61 into eqns. 46 and 47 yields:

$$Z^{\pm} = \frac{abX^{\mp} + [1 - a + ab \mp \bar{\mu}/\mu_0]X^{\pm}}{(1-a)(1-a+2ab) - (\bar{\mu}/\mu_0)^2}$$

where $X^{\pm}$ are given by eqns. 49.

- Note that if we set $b = \frac{1}{2}$ $(g = 0)$ and observe that in this case $X^+ = X^-$, it can be verified that Γ and $Z^{\pm}$ are identical to those terms for the corresponding isotropic scattering (eqns. 10 and 34).
- It is also clear that for $b = \frac{1}{2}$ we recover the earlier result for ρ_∞ (see eqn. 13).
- We determine the constants A and D in eqns. 59–60 from the homogeneous radiation boundary conditions appropriate for the diffuse intensities:

$$A = \frac{(-Z^+ e^{-\tau^*/\mu_0} + Z^- \rho_\infty e^{-\Gamma\tau^*})}{\mathcal{D}}; \qquad D = \frac{(Z^+ \rho_\infty e^{-\tau^*/\mu_0} - Z^- e^{\Gamma\tau^*})}{\mathcal{D}}$$

where $\mathcal{D}$ is defined by eqn. 18.

Two-Stream Solutions for Anisotropic Scattering (4)

- The above solutions satisfy the differential eqns. 46 and 47, and also obey homogeneous boundary conditions.
- It is easy to show that in the limit of **isotropic scattering** the expressions for A and D above reduce to those following eqns. 34 as they should. The solutions for the diffuse intensities are:

$$\begin{aligned} I_d^+ &= \frac{1}{\mathcal{D}}[(-Z^+e^{-\tau/\mu_0} + Z^-\rho_\infty e^{-\Gamma\tau^*})e^{\Gamma\tau} \\ &+ \rho_\infty(Z^+\rho_\infty e^{-\tau^*/\mu_0} - Z^-e^{\Gamma\tau^*})e^{-\Gamma\tau}] + Z^+e^{-\tau/\mu_o} \\ I_d^- &= \frac{1}{\mathcal{D}}[(-Z^+e^{-\tau/\mu_0} + Z^-\rho_\infty e^{-\Gamma\tau^*})\rho_\infty e^{\Gamma\tau} \\ &+ (Z^+\rho_\infty e^{-\tau^*/\mu_0} - Z^-e^{\Gamma\tau^*})e^{-\Gamma\tau}] + Z^-e^{-\tau/\mu_0}. \end{aligned}$$

Light and Life Laboratory STEVENS Institute of Technology

Two-Stream Solutions for Anisotropic Scattering (5)

- We can now solve for the half-range source functions, the flux and the heating rate:

$$S^+(\tau) = a(1-b)I_d^+(\tau) + abI_d^-(\tau) + \frac{aF^s e^{-\tau/\mu_0}}{2\pi} b(\mu_0) \tag{62}$$

$$S^-(\tau) = a(1-b)I_d^-(\tau) + abI_d^+(\tau) + \frac{aF^s e^{-\tau/\mu_0}}{2\pi} [1-b(\mu_0)] \tag{63}$$

$$F(\tau) = 2\pi\bar{\mu}[I_d^+(\tau) - I_d^-(\tau)] - \mu_0 F^s e^{-\tau/\mu_0}. \tag{64}$$

$$\mathcal{H}(\tau) = 2\pi\alpha[I_d^+(\tau) + I_d^-(\tau)] + \alpha F^s e^{-\tau/\mu_0}$$

-

Light and Life Laboratory STEVENS Institute of Technology

Scaling Approximations for Anisotropic Scattering (1)

- In §6.7 we noted that accurate representation of sharply-peaked phase functions typically requires several hundred terms in a Legendre polynomical expansion.
- By making the approximation that photons scattered within this peak are not scattered at all, we found that the RTE becomes more tractable, while losing only a small amount of accuracy.
- This artifice is known as a **scaling approximation**, and takes on various forms depending upon the choice of the truncation.
- We found that in the δ-isotropic approximation the scaled RTE corresponds to an isotropic scattering problem, but with a different optical depth $\hat{\tau} = (1 - af)\tau$ and a different single-scattering albedo $\hat{a} = (1 - f)a/(1 - af)$.
- Here f is the fraction of the phase function within the forward peak. The value of f is somewhat arbitrary, but a good choice is $f = g$, where g is the asymmetry factor. If the remainder of the phase function is constant, the RTE to be solved is:

Scaling Approximations for Anisotropic Scattering

$$\mu \frac{dI^{\pm}(\hat{\tau}, \mu)}{d\tau} = I^{\pm}(\hat{\tau}, \mu) - \frac{\hat{a}}{2} \int_0^1 d\mu' [I^{+}(\hat{\tau}, \mu') + I^{-}(\hat{\tau}, \mu')].$$

- Since we have solved the above equation in the two-stream approximation for three prototype problems, it is a trivial matter to rewrite the solutions in terms of the scaled parameters, $\hat{a}$ and $\hat{\tau}$.
- We will write the asymmetry factor in terms of the backscattering coefficient, $b = (1/2)(1 - g)$. We use as an example the conservative scattering limit, $\hat{a} = 1$ and $\hat{\tau} = 2b\tau$.
- For **Prototype Problem 3** the scaled solutions for the reflectance and transmittance are taken from eqns. 7.98 and 7.99:

$$\rho(-\mu_0, 2\pi) = \frac{2b\tau^* + (\bar{\mu} - \mu_0)(1 - e^{-2b\tau^*/\mu_0})}{2b\tau^* + 2\bar{\mu}} \tag{65}$$

$$\mathcal{T}(\mu_0, 2\pi) = \frac{\bar{\mu} + \mu_0 + (\bar{\mu} - \mu_0)e^{-2b\tau^*/\mu_0}}{2b\tau^* + 2\bar{\mu}}. \tag{66}$$

Accurate Numerical Solutions (1)

More sophisticated approximation techniques include:

- The **discrete-ordinate method**;
- The **spherical-harmonic method**;
- The **doubling-adding method**.
- In "in lowest order" the first two methods become the **two-stream**, and **Eddington approximations**, respectively.

Discrete-Ordinate Method – Isotropic Scattering

Quadrature Formulas

- The solution of the isotropic-scattering problem involves the following integral over angle:

$$\int_{-1}^{1} du\, I(\tau, u) = \int_0^1 d\mu\, I^+(\tau, \mu) + \int_0^1 d\mu\, I^-(\tau, \mu).$$

Accurate Numerical Solutions (2)

- In the two-stream method:

$$\int_{-1}^{1} du\, I \approx I^{+}(\tau) + I^{-}(\tau).$$

- We could improve the accuracy by including more points:

$$\int_{-1}^{1} du\, I(\tau, u) \approx \sum_{j=1}^{m} w'_j I(\tau, u_j)$$

where

- w'_j is a **quadrature weight** and u_j is the **discrete ordinate**.
- The simplest example is the **trapezoidal rule**:

$$\int_{-1}^{1} du\, I \approx \Delta u(\frac{1}{2} I_1 + I_2 + I_3 + \cdots + I_{m-1} + \frac{1}{2} I_m)$$

Light and Life Laboratory STEVENS Institute of Technology

Accurate Numerical Solutions (3)

- The more accurate Simpson's rule is:

$$\int_{-1}^{1} du I \approx \frac{\Delta u}{3}(I_1 + 4I_2 + 2I_3 + 4I_4 + \cdots + I_m)$$

where

- Δu is the (equal) spacing between the adjacent points, u_j, and the I_j denotes $I(\tau, u_j)$.

INTERPOLATION FORMULA

- If we have m points at which we evaluate $I(\tau, u)$, we can replace I with its **approximating polynomial** $\phi(u)$, which is a polynomial of degree $(m-1)$.

Accurate Numerical Solutions (4)

- Consider the following form for $\phi(u)$, for $m = 3$:

$$\begin{aligned}\phi(u) &= I(u_1)\frac{(u-u_2)(u-u_3)}{(u_1-u_2)(u_1-u_3)} + I(u_2)\frac{(u-u_1)(u-u_3)}{(u_2-u_1)(u_2-u_3)} \\ &+I(u_3)\frac{(u-u_1)(u-u_2)}{(u_3-u_1)(u_3-u_2)}.\end{aligned}$$

- $\phi(u)$ is a second-degree polynomial which, when evaluated at the points u_1, u_2, and u_3 yields $I(u_1)$, $I(u_2)$, and $I(u_3)$, respectively.
- This an example of **Lagrange's interpolation formula**. We can write this in abbreviated form, if we use the notation Π to indicate **products** of terms:

$$F(u) \equiv \prod_{j=1}^{m}(u-u_j) = (u-u_1)(u-u_2)\cdots(u-u_m).$$

Light and Life Laboratory STEVENS Institute of Technology

Accurate Numerical Solutions (5)

- Then, since the polynomial $(u-u_1)(u-u_2)\cdots(u-u_{j-1})(u-u_{j+1})\cdots(u-u_m)$ becomes:

$$F(u)/(u-u_j) = \prod_{k\neq j}^{m}(u-u_k)$$

we can write the polynomial $\phi(u)$ in a shorthand form:

$$\phi(u) = \sum_{j=1}^{m} I(u_j)\frac{F(u)}{(u-u_j)F'(u_j)}$$

where $F'(u_j)$ is defined as $dF/du\rfloor_{u=u_j}$.

- The derivative will give a long string of polynomials of degree $(m-1)$; however, when it is evaluated at $u = u_j$, all terms become zero except the term $(u-u_1)(u-u_2)\cdots(u-u_{j-1})(u-u_{j+1})\cdots(u-u_m)$.

Accurate Numerical Solutions (6)

- Hence, the quadrature formula arising from the assumption that the intensity is a polynomial of degree $(m-1)$ is:

$$\int_{-1}^{1} du\ I(u) = \sum_{j=1}^{m} w_j' I(u_j); \qquad w_j' = \frac{1}{F'(u_j)} \int_{-1}^{1} \frac{du\, F(u)}{(u-u_j)}.$$

The quadrature points u_j are, so far, arbitrary.

- The error incurred by using the Lagrange interpolation formula is proportional to the m^{th} derivative of the functions $[I(u)]$ being approximated.*
- Thus, it is clear that *if* $I(\tau, u)$ happens to be a polynomial of degree $(m-1)$ or smaller, then the m-point quadrature formula is exact.

*See, e. g., Burden, R. L., and J. D. Faires, *Numerical Analysis*, Prindle, Weber and Schmidt, Third Edition, Boston, 1985, p. 153.

Example: Simple Demonstration of Quadrature

Let's assume that the intensity is a polynomial of degree 3:

$$I(u) = a_0 + a_1 u + a_2 u^2 + a_3 u^3 \tag{1}$$

where a_i $(i = 0, \ldots, 3)$ are constants.

- Evaluating the function at the points $u_1 = -1$, $u_2 = 0$, and $u_3 = 1$ yields three evenly spaced points in the interval $[-1, 1]$.
- We find $I(u_1) = a_0 - a_1 + a_2 - a_3$, $I(u_2) = a_0$, and $I(u_3) = a_0 + a_1 + a_2 + a_3$.

Accurate Numerical Solutions (8)

- Thus, the approximating polynomial becomes:

$$
\begin{aligned}
\phi(u) &= \frac{1}{2}\left(a_0 - a_1 + a_2 - a_2\right)\left(u^2 - u\right) + a_0(u^2 - 1) + \frac{1}{2}\left(a_0 + a_1 + a_2 + a_3\right)\left(u^2 + u\right) \\
F(u) &= (u - u_1)(u - u_2)(u - u_3) \\
&= u^3 - (u_1 + u_2 + u_3)u^2 + (u_1u_2 + u_1u_3 + u_2u_3)u - u_1u_2u_3 \\
F'(u) &= (u - u_2)(u - u_3) + (u - u_1)(u - u_3) + (u - u_1)(u - u_2)
\end{aligned}
$$

and the quadrature weights become:

$$
w_1' = \frac{1}{F'(u_1)} \int_{-1}^{1} \frac{du\,F(u)}{u - u_1} = \frac{1}{(u_1 - u_2)(u_1 - u_3)} \int_{-1}^{1} (u - u_2)(u - u_3)du = \frac{1}{3}
$$

and similarly:

$$
w_2' = \frac{1}{F'(u_2)} \int_{-1}^{1} \frac{du\,F(u)}{u - u_2} = \frac{4}{3} \qquad \text{and} \qquad w_3' = \frac{1}{F'(u_3)} \int_{-1}^{1} \frac{du\,F(u)}{u - u_3} = \frac{1}{3}.
$$

Accurate Numerical Solutions (9)

So clearly:

$$\int_{-1}^{1} du\ I(u) = \sum_{i=1}^{3} w_i' I(u_i) = \frac{1}{3}\left[I(u_1) + 4I(u_2) + I(u_3)\right] = 2a_o + \frac{2}{3}a_2$$

which is the same as the exact result

$$\int_{-1}^{1} du\ I(u) = \int_{-1}^{1} du\ (a_0 + a_1 u + a_2 u^2 + a_3 u^3) = \left[a_0 u + a_1\frac{u^2}{2} + a_2\frac{u^3}{3} + a_3\frac{u^4}{4}\right]_{-1}^{1} = 2a_0 + \frac{2}{3}a_2$$

- Thus, we have demonstrated that Lagrange's 3-point formula integrates exactly a polynomial of degree 3 or less.
- The error in the Lagrange interpolation polynomial of degree $(m-1)$ is proportional to the m^{th} derivative of the function being approximated.
- The resulting **Newton-Cotes formulas** rely on using even spacing between the points at which the function is evaluated.

Light and Life Laboratory STEVENS Institute of Technology

Accurate Numerical Solutions (10)

We may ask:

- **Is it possible to obtain higher accuracy?** Can this be accomplished by choosing the quadrature points in an optimal manner?

Gauss showed that:

- If $F(u)$ is a certain polynomial, and the u_j are the roots of that polynomial, then we get the accuracy of a polynomial of degree $(2m-1)$.
- This polynomial is the **Legendre polynomial** $P_m(u)$. They have the special property of being orthogonal to every power of u less than m, *i. e.*

As we have seen earlier:

$$\int_{-1}^{1} du\, P_m(u) u^l = 0 \qquad (l = 0, 1, 2, \cdots, m-1).$$

- Note that if u_j is a root of an even Legendre polynomial, then $-u_j$ is also a root. Also, all m roots are real.

Accurate Numerical Solutions (11)

The Double-Gauss Method

- It is customary to choose the **even-order** Legendre polynomials as the approximating polynomial. This choice is made because:
- The roots of the even-orders appear in **pairs**: if we use a negative index to label points in the downward hemisphere and a positive index for points in the upper hemisphere, then $u_{-i} = -u_{+i}$.
- The quadrature weights are the same in each hemisphere, *i. e.* $w'_i = w'_{-i}$.
- The 'full-range' approach has certain problems because it assumes that $I(\tau, u)$ is a smoothly-varying function of u $(-1 \leq u \leq +1)$ with no "sharp corners" for all values of τ.
- For small τ, the intensity changes rather rapidly as u passes through zero, *i. e.* as the line of sight passes through the horizontal. In fact at $\tau = 0$, this change is quite abrupt: $I(\tau = 0, u) = 0$ for slightly negative u-values; for slightly positive u-values it will generally have a finite value.

Light and Life Laboratory STEVENS Institute of Technology

Accurate Numerical Solutions (12)

- It is difficult to 'fit' such a discontinuous distribution with a low-order polynomial that span the full range between $u = -1$ and $u = 1$. It is most difficult to get accurate solutions near the surface: **we should pay the most attention to this region.**

To remedy this situation, the **'Double-Gauss' method** was devised. In this method, the hemispheres are treated separately:

- Instead of approximating $\frac{1}{2}\int_{-1}^{1} du I(u)$ by the sum $\frac{1}{2}\Sigma_{i=-N}^{+N} w_i' I(u_i)$, we break the angular integration into two hemispheres, and approximate each integral separately:

$$\int_{-1}^{1} du\, I = \int_0^1 d\mu\, I^+ + \int_0^1 d\mu\, I^- \approx \sum_{j=1}^{M} w_j I^+(\mu_j) + \sum_{j=1}^{M} w_j I^-(\mu_j).$$

- The w_j and μ_j are the weights and roots of the approximating polynomial for the half-range. Note that we have used the **same** set of weights and roots for both hemispheres.

Accurate Numerical Solutions (13)

- To obtain the highest accuracy, we must again use **Gaussian quadrature.** However, our new interval is $(0 \leq \mu \leq 1)$ instead of $(-1 \leq u \leq 1)$.
- This is easily arranged by defining the variable $u = 2\mu - 1$, so that the orthogonal polynomial is $P_M(2\mu - 1)$.

The new quadrature weight is given by:

$$w_j = \frac{1}{P'_M(2\mu_j - 1)} \int_0^1 d\mu \frac{P_M(2\mu - 1)}{(\mu - \mu_j)} \qquad (2)$$

and the μ_j are the roots of the half-range polynomials.

- Algorithms to compute the roots and weights are usually based on the full range:
- Must relate the half-range quadrature points and weights to those for the full range.

Light and Life Laboratory STEVENS Institute of Technology

Accurate Numerical Solutions (14)

- Since the linear transformation $t = (2x - x_1 - x_2)/(x_2 - x_1)$ will map any interval $[x_1, x_2]$ into $[-1, 1]$ provided $x_2 > x_1$, Gaussian quadrature can be used to approximate:

$$\int_{x_1}^{x_2} dx I(x) = \int_{-1}^{1} dt I\left(\frac{(x_2 - x_1)t + x_2 + x_1}{2}\right)\frac{x_2 - x_1}{2}.$$

Choosing $x_1 = 0$, $x_2 = 1$, $x = \mu$ and $t = u$, we find:

$$\int_0^1 d\mu I(\mu) = \frac{1}{2}\int_{-1}^{1} du I\left(\frac{u+1}{2}\right)$$

and by applying Gaussian quadrature to each integral, we find on setting $M = 2N$ for the half-range:

$$\int_0^1 d\mu I(\mu) = \sum_{j=1}^{2N} w_j I(\mu_j) = \frac{1}{2}\int_{-1}^{1} du I\left(\frac{u+1}{2}\right) = \frac{1}{2}\sum_{\substack{j=-N\\ j\neq 0}}^{N} w'_j I\left(\frac{u_j+1}{2}\right). \quad (3)$$

Light and Life Laboratory
STEVENS Institute of Technology

Accurate Numerical Solutions (15)

- Thus, in even orders the half-range points and weights are related to the full-range ones by:

$$\mu_j = \frac{u_j + 1}{2}; \qquad w_j = \frac{1}{2} w'_j. \tag{4}$$

- The new double-Gauss weights in even orders are half the Gaussian weights in half the order.

- According to eqn. 4 each pair of roots $\pm |u_j|$ for any order N (full-range) generates two positive roots $\mu_j = (-|u_j| + 1)/2$ and $\mu_{2N+1-j} = (|u_j| + 1)/2$ of order $2N$ (half-range).

Accurate Numerical Solutions (16)

Example: Low-order Quadrature

Let's examine the $M = 1$ approximation to see if we retrieve the two-stream approximation.

Consider μ_1, which is $(1 + u_1)/2$.

- Now u_1 is the root of $P_1(u) = u$. This gives $u_1 = 0$, and hence $\mu_1 = \frac{1}{2}$.
- The weight w_1 is easily determined from its definition in eqn. 2:

$$w_1 = \frac{1}{P_1'(2\mu_1 - 1)} \int_0^1 \frac{d\mu(2\mu - 1)}{(\mu - \frac{1}{2})} = 2/P_1'(\mu_1).$$

- Since $P_1 = 2\mu - 1$, $P_1' = 2$, and hence $w_1 = 1$.
- Thus, we retrieve, in the lowest-order double-Gauss formula, the same equations as the two-stream **Schuster-Schwarzschild** equations, in which $\bar{\mu} = 1/2$.

Light and Life Laboratory STEVENS Institute of Technology

Accurate Numerical Solutions (17)

Following the same equations for the lowest *even-order* Gauss formula, we obtain:

- The same expressions except that $\bar{\mu} = 1/\sqrt{3}$, rather than $1/2$.
- This follows since the lowest-order even Gauss formula refers to the $P_2(u) = \frac{1}{2}(3u^2 - 1)$ Legendre polynomial for which $P_2(u) = 0$ for $u_1 = \pm 1/\sqrt{3}$.
- In summary, the lowest-order Double-Gauss formula leads to the 'half-range' two-stream Schuster-Schwarzschild equations; and the lowest-order (even) Gauss formula leads to the 'full-range' two-stream or Eddington approximation.
- We may now use the formulas given above to find the half-range roots and weights for $N = 1$.
- Since the corresponding full-range roots and weights are $u_{\pm 1} = \pm 1/\sqrt{3}$ and $w'_{\pm 1} = 1$, respectively, we find:
- $\mu_1 = \frac{1}{2}(1 - 1/\sqrt{3})$, $\mu_2 = \frac{1}{2}(1 + 1/\sqrt{3})$, $w_1 = \frac{1}{2}$, $w_2 = \frac{1}{2}$ for the half-range roots and weights for $0 < \mu < 1$. For $-1 < \mu < 0$ the weights are the same and $\mu_{-i} = -\mu_i$.

The relationship between **full-range Gaussian** quadrature (u_j, w'_j) and **half-range double-Gaussian** quadrature:

N	j	$2N+1-j$	u_j	w'_j	μ_j	w_j	μ_{2N+1-j}	w_{2N+1-j}
1	1	2	0.57735	1.00000	0.21132	0.50000	0.78868	0.50000
2	1	4	0.33998	0.65215	0.06943	0.17393	0.93057	0.17393
	2	3	0.86114	0.34785	0.33001	0.32607	0.66999	0.32607
3	1	6	0.23862	0.46791	0.03377	0.08566	0.96623	0.08566
	2	5	0.66121	0.36076	0.16940	0.18038	0.83060	0.18038
	3	4	0.93247	0.17132	0.38069	0.23396	0.61931	0.23396
4	1	8	0.18343	0.36268	0.01986	0.05061	0.98014	0.05061
	2	7	0.52553	0.31371	0.10167	0.11119	0.89833	0.11119
	3	6	0.79667	0.22238	0.23723	0.15685	0.76277	0.15685
	4	5	0.96029	0.10123	0.40828	0.18134	0.59172	0.18134
5	1	10	0.14887	0.29552	0.01305	0.03334	0.98695	0.03334
	2	9	0.43340	0.26927	0.06747	0.07473	0.93253	0.07473
	3	8	0.67941	0.21909	0.16030	0.10954	0.83970	0.10954
	4	7	0.86506	0.14945	0.28330	0.13463	0.71670	0.13463
	5	6	0.97391	0.06667	0.42556	0.14776	0.57444	0.14776
6	1	12	0.12523	0.24915	0.00922	0.02359	0.99078	0.02359
	2	11	0.36783	0.23349	0.04794	0.05347	0.95206	0.05347
	3	10	0.58732	0.20317	0.11505	0.08004	0.88495	0.08004
	4	9	0.76990	0.16008	0.20634	0.10158	0.79366	0.10158
	5	8	0.90412	0.10694	0.31608	0.11675	0.68392	0.11675
	6	7	0.98156	0.04718	0.43738	0.12457	0.56262	0.12457

Accurate Numerical Solutions (19)

Anisotropic Scattering

- We will generalize the **discrete ordinate method** to anisotropic scattering in finite inhomogeneous (layered) media.

In doing so we shall introduce a matrix formulation, because it:

- Allows for a compact notation;
- Makes it easy to implement the method numerically;
- This formulation is valid for isotropic scattering as well as for any phase function.

For simplicity we start by considering a homogeneous slab.

- Recall: When the intensity is written as a Fourier cosine series, each Fourier component satisfies a RTE mathematically identical to the azimuthally-averaged equation.
- Thus, we may focus on the RTE for the $m = 0$ component (or the scaled version if we want to utilize the $\delta - M$ scaling).

Accurate Numerical Solutions (20)

- Mathematically the un-scaled and the scaled equations are identical: scaling only influences the optical properties of the medium and will not affect the mathematical solution.
- Therefore, we consider the following pair of equations for the azimuthally-averaged half-range diffuse intensities:

$$\begin{aligned}
\mu\frac{dI^+(\tau,\mu)}{d\tau} &= I^+(\tau,\mu) - \frac{a}{2}\int_0^1 d\mu'\, p(\mu',\mu)I^+(\tau,\mu') \\
&\quad - \frac{a}{2}\int_0^1 d\mu'\, p(-\mu',\mu)I^-(\tau,\mu') - X_0^+ e^{-\tau/\mu_0} \qquad (5)\\
-\mu\frac{dI^-(\tau,\mu)}{d\tau} &= I^-(\tau,\mu) - \frac{a}{2}\int_0^1 d\mu'\, p(\mu',-\mu)I^+(\tau,\mu') \\
&\quad - \frac{a}{2}\int_0^1 d\mu'\, p(-\mu',-\mu)I^-(\tau,\mu') - X_0^- e^{-\tau/\mu_0} \qquad (6)
\end{aligned}$$

where

Light and Life Laboratory
STEVENS Institute of Technology

Accurate Numerical Solutions (21)

$$p(\mu', \mu) = \sum_{l=0}^{2N-1} (2l+1)\chi_l P_l(\mu) P_l(\mu') \tag{7}$$

$$X_0^{\pm} \equiv X_0(\pm\mu) = \frac{a}{4\pi} F^s p(-\mu_0, \pm\mu). \tag{8}$$

We consider the collimated beam case for which:

- we need to deal with the full azimuthal dependence to arrive at the intensity distribution.

The discrete ordinate approximation to the half-range RTE is obtained by:

- Replacing the integrals by quadrature sums and thus transforming the pair of coupled integro-differential into a system of coupled differential equations as follows:

Light and Life Laboratory STEVENS Institute of Technology

Accurate Numerical Solutions (22)

$$\mu_i \frac{dI^+(\tau,\mu_i)}{d\tau} = I^+(\tau,\mu_i) - \frac{a}{2}\sum_{j=1}^{N} w_j p(\mu_j,\mu_i) I^+(\tau,\mu_j) - \frac{a}{2}\sum_{j=1}^{N} w_j p(-\mu_j,\mu_i) I^-(\tau,\mu_j) - X_{0i}^+ e^{-\tau/\mu_0} \quad (9)$$

$$-\mu_i \frac{dI^-(\tau,\mu_i)}{d\tau} = I^-(\tau,\mu_i) - \frac{a}{2}\sum_{j=1}^{N} w_j p(\mu_j,-\mu_i) I^+(\tau,\mu_j) - \frac{a}{2}\sum_{j=1}^{N} w_j p(-\mu_j,-\mu_i) I^-(\tau,\mu_j) - X_{0i}^- e^{-\tau/\mu_0}. \quad (10)$$

Quadrature Rule

- It is convenient to use the same quadrature in each hemisphere so that $\mu_{-i} = -\mu_i$ and $w_{-i} = w_i$.

Light and Life Laboratory STEVENS Institute of Technology

Accurate Numerical Solutions (23)

- The use of Gaussian quadrature is essential because it ensures that the phase function is correctly normalized, i. e.:

$$\sum_{\substack{j=-N \\ j\neq 0}}^{N} w_j p(\tau, \mu_i, \mu_j) = \sum_{\substack{i=-N \\ i\neq 0}}^{N} w_i p(\tau, \mu_i, \mu_j) = 1. \tag{11}$$

Note that:

- Energy is conserved in the computation (no spurious absorption for $a = 1$), because the Gaussian rule is based on the zeros of the Legendre polynomials which we have also used for our expansion of the phase function.

Big Advantages of Expanding the the Phase Function in Legendre Polynomials are:

- (i) **Normalization holds in all orders of approximation**, i. e., for arbitrary values of N; (ii) the "isolation" of the azimuth dependence is accomplished.

Accurate Numerical Solutions (24)

Recall:

- The quadrature points and weights of the "Double-Gauss" scheme satisfy $\mu_{-j} = -\mu_j$, and $w_{-j} = w_j$.

The Main Advantage of this "Double-Gauss" Scheme is that:

- The quadrature points (in even orders) are distributed symmetrically around $|u| = 0.5$ and clustered both towards $|u| = 1$ and $|u| = 0$,

WHEREAS

- In the Gaussian scheme for the complete range, $-1 < u < 1$, they are clustered towards $u = \pm 1$.
- The clustering towards $|u| = 0$ will give superior results near the boundaries where the intensity varies rapidly around $|u| = 0$.
- A half range scheme is also preferable since the intensity is discontinuous at the boundaries.

- Another advantage is that half-range quantities such as upward and downward fluxes and average intensities are obtained immediately without any further approximations.
- Computation of **half-range** quantities using a **full-range** quadrature scheme is obviously **not** self-consistent.

Matrix Formulation of the Discrete-Ordinate Method

- Before we consider the general multi-stream solution, we shall first describe the two-and four-stream cases ($N = 1$ and 2).

Two-stream approximation ($N = 1$):

The two-stream approximation is obtained by:

- Setting $N = 1$ in the half-range RTE, which yields 2 coupled differential equations:

Accurate Numerical Solutions (26)

$$\mu_1 \frac{dI^+(\tau)}{d\tau} = I^+(\tau) - \frac{a}{2}p(-\mu_1, \mu_1)I^-(\tau) - \frac{a}{2}p(\mu_1, \mu_1)I^+(\tau) - Q'^+(\tau) \qquad (12)$$

$$-\mu_1 \frac{dI^-(\tau)}{d\tau} = I^-(\tau) - \frac{a}{2}p(-\mu_1, -\mu_1)I^-(\tau) - \frac{a}{2}p(\mu_1, -\mu_1)I^+(\tau) - Q'^-(\tau) \qquad (13)$$

where

$$\begin{aligned} I^\pm(\tau) &\equiv I^\pm(\tau, \mu_1) \\ Q'^\pm(\tau) &\equiv \frac{a}{4\pi}F^s p(-\mu_0, \pm\mu_1)e^{-\tau/\mu_0} \\ \frac{a}{2}p(\mu_1, -\mu_1) &\equiv \frac{a}{2}(1 - 3g\mu_1^2) \equiv ab = \frac{a}{2}p(-\mu_1, \mu_1) \\ \frac{a}{2}p(\mu_1, \mu_1) &\equiv \frac{a}{2}(1 + 3g\mu_1^2) \equiv a(1-b) = \frac{a}{2}p(-\mu_1, -\mu_1). \end{aligned}$$

Light and Life Laboratory STEVENS Institute of Technology

Accurate Numerical Solutions (27)

Recall that:

- $b \equiv \frac{1}{2}(1 - 3g\mu_1^2)$ is called the backscatter ratio and that g is the first moment of the phase, commonly referred to as the asymmetry factor.
- If we take $\mu_1 = 3^{-\frac{1}{2}}$, then for $g = -1$ we have complete backscattering ($b = 1$), for $g = 1$ complete forward scattering ($b = 0$), and for $g = 0$ isotropic scattering ($b = \frac{1}{2}$).
- The value $\mu_1 = 3^{-\frac{1}{2}}$ corresponds to Gaussian quadrature for the full-range $[-1, 1]$, while Gaussian quadrature for the half range $[0, 1]$ (referred to as Double-Gauss) yields $\mu_1 = \frac{1}{2}$.

We may rewrite eqns. 12 and 13 in matrix form as:

$$\frac{d}{d\tau}\begin{bmatrix} I^+ \\ I^- \end{bmatrix} = \begin{bmatrix} -\alpha & -\beta \\ \beta & \alpha \end{bmatrix}\begin{bmatrix} I^+ \\ I^- \end{bmatrix} - \begin{bmatrix} Q^+ \\ Q^- \end{bmatrix} \tag{14}$$

where

Light and Life Laboratory STEVENS Institute of Technology

Accurate Numerical Solutions (28)

$$
\begin{aligned}
Q^{\pm} &\equiv \pm\mu_1^{-1} Q'^{\pm} \\
\alpha &\equiv \left[\frac{a}{2} p(\mu_1, \mu_1) - 1\right] / \mu_1 = \left[\frac{a}{2} p(-\mu_1, -\mu_1) - 1\right] / \mu_1 = [a(1-b) - 1]/\mu_1 \\
\beta &\equiv \frac{a}{2} p(\mu_1, -\mu_1)/\mu_1 = \frac{a}{2} p(-\mu_1, \mu_1)/\mu_1 = ab/\mu_1.
\end{aligned}
$$

Example 8.3 Four-stream approximation ($N = 2$):

In this case we obtain **four** coupled differential equations:

$$
\begin{aligned}
\mu_1 \frac{dI^+(\tau,\mu_1)}{d\tau} &= I^+(\tau,\mu_1) - Q'^+(\tau,\mu_1) \\
&\quad -w_2\frac{a}{2}p(-\mu_2,\mu_1)I^-(\tau,\mu_2) - w_1\frac{a}{2}p(-\mu_1,\mu_1)I^-(\tau,\mu_1) \\
&\quad -w_1\frac{a}{2}p(\mu_1,\mu_1)I^+(\tau,\mu_1) - w_2\frac{a}{2}p(\mu_2,\mu_1)I^+(\tau,\mu_2) \\
\mu_2 \frac{dI^+(\tau,\mu_2)}{d\tau} &= I^+(\tau,\mu_2) - Q'^+(\tau,\mu_2) \\
&\quad -w_2\frac{a}{2}p(-\mu_2,\mu_2)I^-(\tau,\mu_2) - w_1\frac{a}{2}p(-\mu_1,\mu_2)I^-(\tau,\mu_1) \\
&\quad -w_1\frac{a}{2}p(\mu_1,\mu_2)I^+(\tau,\mu_1) - w_2\frac{a}{2}p(\mu_2,\mu_2)I^+(\tau,\mu_2) \\
-\mu_1 \frac{dI^-(\tau,\mu_1)}{d\tau} &= I^-(\tau,\mu_1) - Q'^-(\tau,\mu_1) \\
&\quad -w_2\frac{a}{2}p(-\mu_2,-\mu_1)I^-(\tau,\mu_2) - w_1\frac{a}{2}p(-\mu_1,-\mu_1)I^-(\tau,\mu_1) \\
&\quad -w_1\frac{a}{2}p(\mu_1,-\mu_1)I^+(\tau,\mu_1) - w_2\frac{a}{2}p(\mu_2,-\mu_1)I^+(\tau,\mu_2) \\
-\mu_2 \frac{dI^-(\tau,\mu_2)}{d\tau} &= I^-(\tau,\mu_2) - Q'^-(\tau,\mu_2) \\
&\quad -w_2\frac{a}{2}p(-\mu_2,-\mu_2)I^-(\tau,\mu_2) - w_1\frac{a}{2}p(-\mu_1,-\mu_2)I^-(\tau,\mu_1) \\
&\quad -w_1\frac{a}{2}p(\mu_1,-\mu_2)I^+(\tau,\mu_1) - w_2\frac{a}{2}p(\mu_2,-\mu_2)I^+(\tau,\mu_2)
\end{aligned}
$$

Accurate Numerical Solutions (30)

We may rewrite these equations in matrix form as follows:

$$\frac{d}{d\tau}\begin{bmatrix} I^+(\tau,\mu_1) \\ I^+(\tau,\mu_2) \\ I^-(\tau,\mu_1) \\ I^-(\tau,\mu_2) \end{bmatrix} = \begin{bmatrix} -\alpha_{11} & -\alpha_{12} & -\beta_{11} & -\beta_{12} \\ -\alpha_{21} & -\alpha_{22} & -\beta_{21} & -\beta_{22} \\ \beta_{11} & \beta_{12} & \alpha_{11} & \alpha_{12} \\ \beta_{21} & \beta_{22} & \alpha_{21} & \alpha_{22} \end{bmatrix} \begin{bmatrix} I^+(\tau,\mu_1) \\ I^+(\tau,\mu_2) \\ I^-(\tau,\mu_1) \\ I^-(\tau,\mu_2) \end{bmatrix} - \begin{bmatrix} Q^+(\tau,\mu_1) \\ Q^+(\tau,\mu_2) \\ Q^-(\tau,\mu_1) \\ Q^-(\tau,\mu_2) \end{bmatrix} \quad (15)$$

where

$$\begin{aligned}
Q^{\pm}(\tau,\mu_i) &= \pm\mu_i^{-1}Q'^{\pm}(\tau,\mu_i), \qquad i=1,2, \\
\alpha_{11} &= \mu_1^{-1}[w_1\frac{a}{2}p(\mu_1,\mu_1)-1] = \mu_1^{-1}[w_1\frac{a}{2}p(-\mu_1,-\mu_1)-1], \\
\alpha_{12} &= \mu_1^{-1}w_2\frac{a}{2}p(\mu_2,\mu_1) = \mu_1^{-1}w_2\frac{a}{2}p(-\mu_2,-\mu_1), \\
\alpha_{21} &= \mu_2^{-1}w_1\frac{a}{2}p(\mu_1,\mu_2) = \mu_2^{-1}w_1\frac{a}{2}p(-\mu_1,-\mu_2), \\
\alpha_{22} &= \mu_2^{-1}[w_2\frac{a}{2}p(\mu_2,\mu_2)-1] = \mu_2^{-1}[w_2\frac{a}{2}p(-\mu_2,-\mu_2)-1],
\end{aligned}$$

$$
\begin{aligned}
\beta_{11} &= \mu_1^{-1} w_1 \frac{a}{2} p(\mu_1, -\mu_1) = \mu_1^{-1} w_1 \frac{a}{2} p(-\mu_1, \mu_1), \\
\beta_{12} &= \mu_1^{-1} w_2 \frac{a}{2} p(-\mu_2, \mu_1) = \mu_1^{-1} w_2 \frac{a}{2} p(\mu_2, -\mu_1), \\
\beta_{21} &= \mu_2^{-1} w_1 \frac{a}{2} p(-\mu_1, \mu_2) = \mu_2^{-1} w_1 \frac{a}{2} p(\mu_1, -\mu_2), \\
\beta_{22} &= \mu_2^{-1} w_2 \frac{a}{2} p(-\mu_2, \mu_2) = \mu_2^{-1} w_2 \frac{a}{2} p(\mu_2, -\mu_2).
\end{aligned}
$$

By introducing the vectors

$$
\mathbf{I}^{\pm} = \{I^{\pm}(\tau, \mu_i)\}, \qquad \mathbf{Q}^{\pm} = \{Q^{\pm}(\tau, \mu_i)\}, \qquad i = 1, 2
$$

we may write eqn. 15 in a more compact form as:

$$
\frac{d}{d\tau}\begin{bmatrix} \mathbf{I}^+ \\ \mathbf{I}^- \end{bmatrix} = \begin{bmatrix} -\tilde{\alpha} & -\tilde{\beta} \\ \tilde{\beta} & \tilde{\alpha} \end{bmatrix}\begin{bmatrix} \mathbf{I}^+ \\ \mathbf{I}^- \end{bmatrix} - \begin{bmatrix} \mathbf{Q}^+ \\ \mathbf{Q}^- \end{bmatrix} \tag{16}
$$

where all the elements of the matrices $\tilde{\alpha}$ and $\tilde{\beta}$ are defined above.

Note that:

- This equation is very similar to the one obtained in the two-stream approximation except that the scalars α and β have become 2×2 matrices.
- $\tilde{\alpha}$ and $\tilde{\beta}$ may be interpreted as local transmission and reflection operators.

Multi-stream approximation (N arbitrary):

It should now be obvious how to generalize this scheme:

- We write eqn. 9 and 10 in matrix form as:

$$\frac{d}{d\tau}\begin{bmatrix}\mathbf{I}^+\\ \mathbf{I}^-\end{bmatrix} = \begin{bmatrix}-\tilde{\alpha} & -\tilde{\beta}\\ \tilde{\beta} & \tilde{\alpha}\end{bmatrix}\begin{bmatrix}\mathbf{I}^+\\ \mathbf{I}^-\end{bmatrix} - \begin{bmatrix}\mathbf{Q}^+\\ \mathbf{Q}^-\end{bmatrix} \tag{17}$$

where

$$\begin{aligned}
\mathbf{I}^{\pm} &= \{I^{\pm}(\tau,\mu_i)\} \qquad i = 1,\ldots,N\\
\mathbf{Q}^{\pm} &= \pm\mathbf{M}^{-1}\mathbf{Q}'^{\pm} = \{Q^{\pm}(\tau,\mu_i)\} \qquad i = 1,\ldots,N\\
\mathbf{M} &= \{\mu_i\delta_{ij}\} \qquad i,j = 1,\ldots,N\\
\tilde{\alpha} &= \mathbf{M}^{-1}\{\mathbf{D}^+\mathbf{W} - \mathbf{1}\}\\
\tilde{\beta} &= \mathbf{M}^{-1}\mathbf{D}^-\mathbf{W}\\
\mathbf{W} &= \{w_i\delta_{ij}\} \qquad i,j = 1,\ldots,N\\
\mathbf{1} &= \{\delta_{ij}\} \qquad i,j = 1,\ldots,N\\
\mathbf{D}^+ &= \frac{a}{2}\{p(\mu_j,\mu_i)\} = \frac{a}{2}\{p(-\mu_j,-\mu_i)\} \qquad i,j = 1,\ldots,N\\
\mathbf{D}^- &= \frac{a}{2}\{p(-\mu_j,\mu_i)\} = \frac{a}{2}\{p(\mu_j,-\mu_i)\} \qquad i,j = 1,\ldots,N.
\end{aligned}$$

Accurate Numerical Solutions (33)

We note that the structure of the $(2N \times 2N)$ matrix:

$$\begin{bmatrix} -\tilde{\alpha} & -\tilde{\beta} \\ \tilde{\beta} & \tilde{\alpha} \end{bmatrix}$$

in eqn. 17 can be traced to the fact that

- The phase function depends only on the scattering angle (i. e., the angle between $\hat{\Omega}(\mu, \phi)$ and $\hat{\Omega}'(\mu', \phi')$.
- This special structure is also a consequence of having chosen a quadrature rule satisfying $\mu_{-i} = -\mu_i$, $w_{-i} = w_i$.
- Because of this structure, eqn. 17 permits eigensolutions with eigenvalues occurring in positive/negative pairs:
- We can reduce the order of the resulting algebraic eigenvalue problem by a factor of 2 which leads to a decrease of the computational burden by a factor of 8.

Matrix Eigensolutions

Two-stream solutions ($N = 1$):

- Seek solutions to the homogeneous version of eqn. 14 ($Q^{\pm} = 0$) of the form $I^{\pm} = g^{\pm} e^{-\lambda\tau}$, $g^{\pm} = g(\pm\mu_1)$. This leads to the algebraic eigenvalue problem:

$$\begin{bmatrix} \alpha & \beta \\ -\beta & -\alpha \end{bmatrix} \begin{bmatrix} g^+ \\ g^- \end{bmatrix} = \lambda \begin{bmatrix} g^+ \\ g^- \end{bmatrix}. \tag{18}$$

Writing this matrix equation as follows:

$$\begin{aligned} \alpha g^+ + \beta g^- &= \lambda g^+ \\ -\beta g^+ - \alpha g^- &= \lambda g^- \end{aligned}$$

and adding and subtracting these two equations, we find:

$$(\alpha - \beta)(g^+ - g^-) = \lambda(g^+ + g^-) \tag{19}$$

$$(\alpha + \beta)(g^+ + g^-) = \lambda(g^+ - g^-). \tag{20}$$

Accurate Numerical Solutions (35)

Substitution of the last equation into eqn. 19 yields:

$$(\alpha - \beta)(\alpha + \beta)(g^+ + g^-) = \lambda^2 (g^+ + g^-)$$

which has the solutions $\lambda_1 = k$, $\lambda_{-1} = -k$ with

$$k = \sqrt{\alpha^2 - \beta^2} = \frac{1}{\mu_1}\sqrt{(1-a)(1-a+2ab)} > 0 \qquad (a < 1) \tag{21}$$

$$g^+ + g^- = \text{arbitrary constant} \qquad (= 1) \tag{22}$$

which we may set equal to unity.

For $\lambda_1 = k$ eqn. 20 yields:

$$g^+ - g^- = (\alpha + \beta)/k \tag{23}$$

(assuming $k \neq 0$ or $a \neq 1$).

Accurate Numerical Solutions (36)

- Combining eqns. 22 and 23 we find:

$$\frac{g_1^+}{g_1^-} = \frac{k + (\alpha + \beta)}{k - (\alpha + \beta)} = \frac{\sqrt{1 - a + 2ab} - \sqrt{1 - a}}{\sqrt{1 - a + 2ab} + \sqrt{1 - a}} \equiv \rho_\infty. \tag{24}$$

and thus

$$\begin{bmatrix} g_1^+ \\ g_1^- \end{bmatrix} = \begin{bmatrix} \rho_\infty \\ 1 \end{bmatrix} \tag{25}$$

which is the eigenvector belonging to eigenvalue $\lambda_1 = k$.

- Repeating this for $\lambda_{-1} = -k$, we find $g_{-1}^- / g_{-1}^+ = \rho_\infty$, and:

$$\begin{bmatrix} g_{-1}^+ \\ g_{-1}^- \end{bmatrix} = \begin{bmatrix} 1 \\ \rho_\infty \end{bmatrix}. \tag{26}$$

Accurate Numerical Solutions (37)

The complete homogeneous solution becomes a linear combination of the exponential solutions for eigenvalues $\lambda_1 = k$ and $\lambda_{-1} = -k$, i. e.

$$\begin{aligned} I^+(\tau) &= I(\tau, +\mu_1) = C_{-1} g_{-1}(+\mu_1) e^{+k\tau} + C_1 g_1(+\mu_1) e^{-k\tau} \\ &= C_{-1} g_{-1}(+\mu_1) e^{+k\tau} + \rho_\infty C_1 g_1(-\mu_1) e^{-k\tau} \qquad (27) \\ I^-(\tau) &= I(\tau, -\mu_1) = C_{-1} g_{-1}(-\mu_1) e^{+k\tau} + C_1 g_1(-\mu_1) e^{-k\tau} \\ &= \rho_\infty C_{-1} g_{-1}(+\mu_1) e^{+k\tau} + C_1 g_1(-\mu_1) e^{-k\tau} \qquad (28) \end{aligned}$$

where C_1 and C_{-1} are constants of integration. We note that:

- These solutions are identical to those given previously for the two-stream approximation as they should be.
- In anticipation of the extension to more than two streams we may rewrite the solution in the following somewhat artificial form:

$$I^{\pm}(\tau, \mu_i) = \sum_{j=1}^{1} C_{-j} g_{-j}(\pm\mu_i) e^{k_j \tau} + \sum_{j=1}^{1} C_j g_j(\pm\mu_i) e^{-k_j \tau} \qquad i = 1, 1 \qquad (29)$$

with $k_1 = k$, given by eqn. 21.

Accurate Numerical Solutions (38)

Multi-stream solutions (N arbitrary)

- Equations 17 is a system of $2N$ coupled, ordinary differential equations with constant coefficients.
- These coupled equations are linear and our goal is to uncouple them by using well-known methods of linear algebra.
- From the discussion of the two- and four-stream cases it is now obvious that we should proceed by seeking solutions to the homogeneous version ($\mathbf{Q} = 0$) of eqn. 17 of the form:

$$\mathbf{I}^{\pm} = \mathbf{g}^{\pm} e^{-k\tau}. \tag{30}$$

We find:

$$\begin{bmatrix} \tilde{\alpha} & \tilde{\beta} \\ -\tilde{\beta} & -\tilde{\alpha} \end{bmatrix} \begin{bmatrix} \mathbf{g}^{+} \\ \mathbf{g}^{-} \end{bmatrix} = k \begin{bmatrix} \mathbf{g}^{+} \\ \mathbf{g}^{-} \end{bmatrix} \tag{31}$$

- Equation 31 is a standard algebraic eigenvalue problem of order $2N \times 2N$ with eigenvalues k and eigenvectors $\mathbf{g}^{\pm}$.

Accurate Numerical Solutions (39)

- Because of the special structure of the matrix in eqn. 31, the eigenvalues occur in positive/negative pairs and the order of the algebraic eigenvalue problem (eqn. 31) may be reduced as follows:

We rewrite the homogeneous version of eqn. 17 as:

$$\frac{d\mathbf{I}^+}{d\tau} = -\tilde{\alpha}\mathbf{I}^+ - \tilde{\beta}\mathbf{I}^-$$
$$\frac{d\mathbf{I}^-}{d\tau} = \tilde{\alpha}\mathbf{I}^- + \tilde{\beta}\mathbf{I}^+.$$

Adding these two equations, we find:

$$\frac{d(\mathbf{I}^+ + \mathbf{I}^-)}{d\tau} = -(\tilde{\alpha} - \tilde{\beta})(\mathbf{I}^+ - \mathbf{I}^-) \tag{32}$$

Subtracting these two equations, we find:

$$\frac{d(\mathbf{I}^+ - \mathbf{I}^-)}{d\tau} = -(\tilde{\alpha} + \tilde{\beta})(\mathbf{I}^+ + \mathbf{I}^-). \tag{33}$$

Light and Life Laboratory STEVENS Institute of Technology

Accurate Numerical Solutions (40)

Combining eqns. 32 and 33, we obtain:

$$\frac{d^2(\mathbf{I}^+ + \mathbf{I}^-)}{d\tau^2} = (\tilde{\alpha} - \tilde{\beta})(\tilde{\alpha} + \tilde{\beta})(\mathbf{I}^+ + \mathbf{I}^-)$$

or in view of eqn. 30:

$$(\tilde{\alpha} - \tilde{\beta})(\tilde{\alpha} + \tilde{\beta})(\mathbf{g}^+ + \mathbf{g}^-) = k^2(\mathbf{g}^+ + \mathbf{g}^-) \tag{34}$$

- This completes the reduction of the order.
- To proceed we solve eqn. 34 to obtain eigenvalues and eigenvectors $(\mathbf{g}^+ + \mathbf{g}^-)$.
- We then use eqn. 33 to determine $(\mathbf{g}^+ - \mathbf{g}^-)$, and proceed as in the four-stream case to construct a complete set of eigenvectors.

Accurate Numerical Solutions (41)

Inhomogeneous Solution

- It is easily verified that a particular solution for collimated beam incidence is:

$$I(\tau, u_i) = Z_0(u_i) e^{-\tau/\mu_0} \tag{35}$$

where the $Z_0(u_i)$ are determined by the following system of **linear algebraic** equations:

$$\sum_{\substack{j=-N \\ j \neq 0}}^{N} \left[(1 + u_j/\mu_0)\delta_{ij} - w_j \frac{a}{2} p(u_j, u_i) \right] Z_0(u_j) = X_0(u_i). \tag{36}$$

Equation 36 is obtained by simply substituting the “trial” solution (eqn. 35) into eqns. 9–10.

Light and Life Laboratory STEVENS Institute of Technology

Accurate Numerical Solutions (42)

- In the two-stream case eqn. 36 reduces to a system of two algebraic equations with two unknowns which is easily solved analytically and the solutions were provided previously.
- The four-stream case involves four algebraic equations and may also be solved analytically,

BUT

- This may not be worth the effort, since standard linear equation solvers have built-in features like pivoting implying that such a software package is, in general, likely to produce numerical results superior to those obtained from the analytic solutions.

Example: Thermal Source

For thermal sources the emitted radiation is isotropic (and azimuth-independent):

$$Q'(\tau) = (1 - a)B(\tau).$$

Accurate Numerical Solutions (43)

To account for the temperature variation in the slab we may approximate the Planck function for each layer by a polynomial in optical depth τ:

$$B[T(\tau)] = \sum_{l=0}^{K} b_l \tau^l.$$

Then

- if we insist that the solution should also be a polynomial in τ, i. e.

$$I(\tau, u_i) = \sum_{l=0}^{K} Y_l(u_i)\tau^l$$

- we can show that the coefficients $Y_l(u_i)$ are determined by solving the following system of linear algebraic equations:

$$\begin{aligned} Y_K(u_i) &= (1-a)b_K \\ \sum_{j=-N}^{N} \left(\delta_{ij} - w_j \frac{a}{2} p(u_j, u_i)\right) Y_l(u_j) &= (1-a)b_l - (l+1)u_i Y_{l+1}(u_i) \\ & \quad l = K-1, K-2, \ldots, 0. \end{aligned}$$

Accurate Numerical Solutions (44)

- It is popular to use a linear approximation ($K = 1$), which only requires knowledge of the temperature at layer interfaces to compute the Planck function there.
- Noting that the Planck function depends **linearly** on temperature in the long wavelength (Rayleigh-Jeans) limit, but **exponentially** in the short wavelength (Wien's) limit:
- we expect an **exponential times a linear** dependence of the Planck function on τ to work well under most circumstances.

General Solution

The general solution to eqns. 9 and 10 consists of a linear combination, with coefficients C_j, of all the homogeneous solutions, plus the particular solution:

$$I^{\pm}(\tau, \mu_i) = \sum_{j=1}^{N} C_{-j} g_{-j}(\pm\mu_i) e^{k_j \tau} + \sum_{j=1}^{N} C_j g_j(\pm\mu_i) e^{-k_j \tau}$$
$$+Z_0(\pm\mu_i) e^{-\tau/\mu_0} \qquad i = 1, \ldots, N. \tag{37}$$

Light and Life Laboratory STEVENS Institute of Technology

Accurate Numerical Solutions (45)

Recall that:

- The k_j and $g_j(\pm\mu_i)$ are the eigenvalues and eigenvectors obtained as described above.
- The $\pm\mu_i$ are the quadrature angles.
- The $C_{\pm j}$ the constants of integration.

Source Function and Angular Distributions

For a slab of thickness τ^*, we may solve eqns. 9 and 10 formally to obtain ($\mu > 0$):

$$I^+(\tau,\mu) = I^+(\tau^*,\mu)e^{-(\tau^*-\tau)/\mu} + \int_\tau^{\tau^*} \frac{dt}{\mu} S^+(t,\mu)e^{-(t-\tau)/\mu} \tag{38}$$

$$I^-(\tau,\mu) = I^-(0,\mu)e^{-\tau/\mu} + \int_0^{\tau} \frac{dt}{\mu} S^-(t,\mu)e^{-(\tau-t)/\mu}. \tag{39}$$

Light and Life Laboratory STEVENS Institute of Technology

Accurate Numerical Solutions (46)

These two equations show that:

- If we know the source function $S^{\pm}(t, \mu)$, we can find the intensity at arbitrary angles by integrating the source function.
- We shall use the discrete ordinate solutions to derive explicit expressions for the source function which can be integrated analytically.

Analytic Expression for the Source Function

- In view of eqns. 9–10 the discrete-ordinate approximation to the source function may be written as:

$$\begin{aligned} S^{\pm}(\tau, \mu) &= \frac{a}{2} \sum_{i=1}^{N} w_i p(-\mu_i, \pm\mu) I^{-}(\tau, \mu_i) \\ &+ \frac{a}{2} \sum_{i=1}^{N} w_i p(+\mu_i, \pm\mu) I^{+}(\tau, \mu_i) + X_0^{\pm}(\mu) e^{-\tau/\mu_0}. \end{aligned} \tag{40}$$

Accurate Numerical Solutions (47)

Substituting the general solution of eqn. 37 into eqn. 40, we find:

$$S^{\pm}(\tau,\mu) = \sum_{j=1}^{N} C_{-j}\tilde{g}_{-j}(\pm\mu)e^{k_j\tau} + \sum_{j=1}^{N} C_j\tilde{g}_j(\pm\mu)e^{-k_j\tau} + \tilde{Z}_0^{\pm}(\mu)e^{-\tau/\mu_0} \qquad (41)$$

where

$$\tilde{g}_j(\pm\mu) = \frac{a}{2}\sum_{i=1}^{N}\{w_i p(-\mu_i,\pm\mu)g_j(-\mu_i) + w_i p(+\mu_i,\pm\mu)g_j(+\mu_i)\} \qquad (42)$$

$$\tilde{Z}_0^{\pm}(\mu) = \frac{a}{2}\sum_{i=1}^{N}\{w_i p(-\mu_i,\pm\mu)Z_0(-\mu_i) + w_i p(+\mu_i,\pm\mu)Z_0(+\mu_i)\} + X_0(\pm\mu). \qquad (43)$$

Note that:

- Equations 42 and 43 are convenient analytic interpolation formulas for the $\tilde{g}_j(\pm\mu)$ and the $\tilde{Z}_0(\pm\mu)$.
- They clearly reveal the interpolatory nature of eqn. 41 for the source function.
- The fact that they are derived from the basic radiative transfer equation to which we are seeking solutions, indicates that these expressions may be superior to any other standard interpolation scheme.

Accurate Numerical Solutions (48)

Interpolated Intensities

Using eqns. 41 in eqns. 38–39, we find that for a layer of thickness τ^*, the intensities become:

$$I^+(\tau,\mu) = I^+(\tau^*,\mu)e^{-(\tau^*-\tau)/\mu} + \sum_{j=-N}^{N} C_j \frac{\tilde{g}_j(+\mu)}{1+k_j\mu}\left\{e^{-k_j\tau} - e^{-[k_j\tau^*+(\tau^*-\tau)/\mu]}\right\} \quad (44)$$

$$I^-(\tau,\mu) = I^-(0,\mu)e^{-\tau/\mu} + \sum_{j=-N}^{N} C_j \frac{\tilde{g}_j(-\mu)}{1-k_j\mu}\left\{e^{-k_j\tau} - e^{-\tau/\mu}\right\} \quad (45)$$

- We have for convenience included the particular solution as the $j = 0$ term in the sum so that $C_0\tilde{g}_0(\pm\mu) \equiv \tilde{Z}_0(\pm\mu)$ and $k_0 \equiv 1/\mu_0$.
- The basic soundness and merit of the intensity expressions given above will be demonstrated in the following examples.

Accurate Numerical Solutions (49)

- First, we note that eqns. 44–45 when evaluated at the quadrature points, yield results identical to eqns. 37.
- Secondly, eqns. 44–45 satisfy the boundary conditions for all μ-values (even though we have imposed such conditions only at the quadrature points!).
- Thirdly, the more complicated expressions (i. e. eqns. 44–45 as compared to eqn. 37) have the merit of "correcting" the simpler expression (eqn. 37) for μ-values not coinciding with the quadrature points.

Example: The Merit of the Interpolation Scheme

- Equations 44 and 45 provide a convenient means of computing the intensities:
- **for arbitrary angles AND at any desired optical depth.**

However:

- the merit of these expressions depends crucially on the ability to compute efficiently the eigenvectors $\tilde{g}_j(\pm\mu)$ and the particular solution vector $\tilde{Z}_0(\pm\mu)$.

Accurate Numerical Solutions (50)

- Since the $g_j(\mu)$ are known at the quadrature points ($\mu = \mu_i, i = \pm 1, \ldots, \pm N$), this information can be used as a basis for interpolation using any standard interpolation scheme.

The following figure illustrates the problems one might encounter in interpolation using standard techniques:

- The eigenvector corresponding to the smallest eigenvalue for a phase function typical of atmospheric aerosols with single scattering albedo $a = 0.9$ illustrates the typical behavior of some of the eigenvectors.
- A 16-stream computation ($N = 8$) was used in this example. The values at the quadrature points to be interpolated are indicated by the dots.
- We notice that there is a pronounced dip close to $\mu = 0$.
- It is difficult to fit a polynomial to a function with such a pronounced dip. A cubic spline interpolation also performs poorly on both sides of the dip, whereas the analytic expression (eqn. 42) yields good results.

Accurate Numerical Solutions (51)

Consequence of using Different Interpolation Schemes:

- The analytic expressions to compute the eigenvectors and the particular solution vector yield good results.
- The results obtained by using cubic spline interpolation of the eigenvectors are inaccurate for $-0.6 < u < -0.1$.

This example illustrates that:

- An interpolation scheme which interpolates the eigenvectors, is best suited as a general purpose interpolation scheme: because:
- it can provide accurate intensities at any desired angle and depth.

Accurate Numerical Solutions (52)

Boundary Conditions – Removal of Ill-Conditioning

Boundary Conditions

We noted that:

- If the diffuse bidirectional reflectance, $\rho_d(\mu, \phi; -\mu', \phi')$, is a function only of the difference between the azimuthal angles before and after reflection, then we may expand it in a cosine series as follows:

$$\rho_d(-\mu', \phi'; \mu, \phi) = \rho_d(-\mu', \mu; \phi - \phi') = \sum_{m=0}^{2N-1} \rho_d^m(-\mu', \mu) \cos m(\phi - \phi')$$

where the expansion coefficients are computed from:

$$\rho_d^m(-\mu', \mu) = \frac{1}{\pi} \int_{-\pi}^{\pi} d(\phi - \phi') \rho_d(-\mu', \mu; \phi - \phi') \cos m(\phi - \phi').$$

Here the superscript m refers to the azimuthal component.

Light and Life Laboratory STEVENS Institute of Technology

Accurate Numerical Solutions (53)

- The advantage of this expansion is that we again are able to isolate the azimuthal components. In fact, each Fourier component must satisfy the bottom boundary condition:

$$\begin{aligned} I^m(\tau^*, +\mu) &= \delta_{m0}\epsilon(\mu)B(T_s) + (1+\delta_{m0})\int_0^1 d\mu'\ \mu'\rho_d^m(-\mu', \mu)I^m(\tau^*, -\mu') \\ &\quad + \frac{\mu_0 F^s}{\pi} e^{-\tau^*/\mu_0}\rho_d^m(\mu, -\mu_0) \qquad (46) \\ &\equiv I_s^m(\mu). \end{aligned}$$

where T_s is the temperature of, and $\epsilon(\mu)$ is the emittance of the lower boundary surface.

Thus, eqns. 37 must satisfy boundary conditions as follows:

$$I^m(0, -\mu_i) = \mathcal{I}^m(-\mu_i), \qquad i = 1, \ldots, N \qquad (47)$$

$$I^m(\tau^*, +\mu_i) = I_s^m(\mu_i), \qquad i = 1, \ldots, N \qquad (48)$$

Accurate Numerical Solutions (54)

where

$$I_s^m(\mu_i) = \delta_{m0}\epsilon(\mu_i)B(T_s) + (1+\delta_{m0})\sum_{j=1}^{N} w_j\mu_j\rho_d^m(\mu_i,-\mu_j)I^m(\tau^*,-\mu_j)$$
$$+\frac{\mu_0 F^s}{\pi}e^{-\tau^*/\mu_0}\rho_d^m(\mu_i,-\mu_0). \qquad (49)$$

$\mathcal{I}^m(-\mu_i)$ is the radiation incident at the top boundary.

Note that:

- For *Prototype Problem 1* we would have $\mathcal{I}^m(-\mu_i) =$ constant (the same for all μ_i) for $m = 0$, and $\mathcal{I}^m(-\mu_i) = 0$ for $m \neq 0$ (uniform illumination).
- For **Prototype Problems 2 and 3** we have, of course, $\mathcal{I}^m(-\mu_i) = 0$ since there is by definition no diffuse radiation incident in **Prototype Problem 3** and **Prototype Problem 2** is assumed to be driven entirely by internal radiation sources.

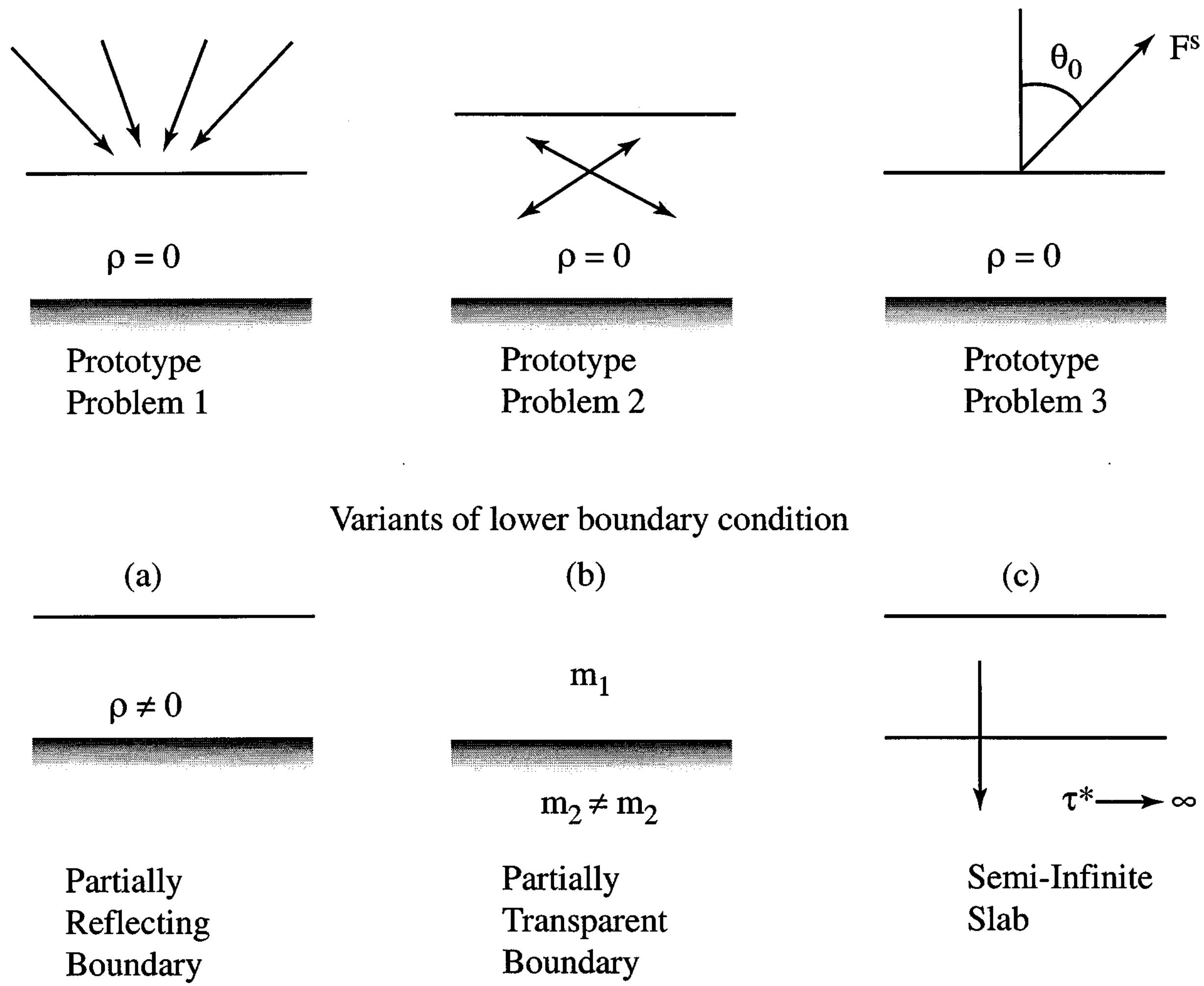

Figure 1: Illustration of Prototype Problems in radiative transfer.

Accurate Numerical Solutions (56)

Note also that:

- Since eqns. 47 and 48 introduce a fundamental distinction between downward directions (denoted by $-$) and upward directions (denoted by $+$), one should select a quadrature rule which integrates separately over the downward and upward directions.
- As noted previously, the Double-Gauss rule that we have adopted satisfies this requirement.

For the discussion of boundary conditions, it is convenient to write the discrete ordinate solution in the following form ($k_j > 0$ and $k_{-j} = -k_j$):

$$I^{\pm}(\tau, \mu_i) = \sum_{j=1}^{N} \left[C_j g_j(\pm\mu_i) e^{-k_j \tau} + C_{-j} g_{-j}(\pm\mu_i) e^{+k_j \tau} \right] + U^{\pm}(\tau, \mu_i) \qquad (50)$$

Here:

- The sum contains the homogeneous solution involving the unknown coefficients (the C_j) and
- $U^{\pm}(\tau, \mu_i)$ is the particular solution given by eqn. 35.

Accurate Numerical Solutions (57)

Insertion of eqn. 50 into eqns. 47–49 yields (omitting the m-superscript):

$$\sum_{j=1}^{N} \{C_j g_j(-\mu_i) + C_{-j} g_{-j}(-\mu_i)\} = \mathcal{I}(-\mu_i) - U^-(0, \mu_i), \qquad i = 1, \ldots, N \quad (51)$$

$$\begin{aligned} \sum_{j=1}^{N} \left\{C_j r_j(\mu_i) g_j(+\mu_i) e^{-k_j \tau^*} + C_{-j} r_{-j}(\mu_i) g_{-j}(+\mu_i) e^{k_j \tau^*}\right\} &= \Gamma(\tau^*, \mu_i), \\ i &= 1, \ldots, N \end{aligned} \quad (52)$$

where

$$r_j(\mu_i) = 1 - (1 + \delta_{m0}) \sum_{n=1}^{N} \rho_d(\mu_i, -\mu_n) w_n \mu_n g_j(-\mu_n) / g_j(+\mu_i) \quad (53)$$

$$\begin{aligned} \Gamma(\tau^*, \mu_i) &= \delta_{m0} \epsilon(\mu_i) B(T_s) - U^+(\tau^*, \mu_i) \\ &\quad + (1 + \delta_{m0}) \sum_{j=1}^{N} \rho_d(\mu_i, -\mu_j) w_j \mu_j U^-(\tau^*, \mu_j) \\ &\quad + \frac{\mu_0 F^s}{\pi} e^{-\tau^*/\mu_0} \rho_d(\mu_i, -\mu_0). \end{aligned} \quad (54)$$

Note that:

- Equations 51 and 52 constitute a $2N \times 2N$ system of linear algebraic equations from which the $2N$ unknown coefficients, the C_j ($j = \pm 1, \ldots, \pm N$) are determined.

Removal of Numerical Ill-Conditioning

- The numerical solution of this set of equations is seriously hampered by the fact that eqns. 51 and 52 are intrinsically ill-conditioned.

By "ill-conditioning" we mean:

- When eqns. 51 and 52 are written in matrix form the resulting matrix cannot be successfully inverted by existing computers that work with "finite-digit" arithmetic.
- If τ^* is sufficiently large, som of the elements of the matrix become huge while others become tiny, and it is this situation that leads to ill-conditioning.

Accurate Numerical Solutions (59)

- Fortunately, this ill-conditioning may be entirely eliminated by a simple scaling transformation discussed below.

Attempts to solve eqns. 51 and 52 as they stand reveal that they are notoriously ill-conditioned:

- The root of the ill-conditioning problem lies in the occurrence of exponentials with positive arguments in eqns. 51 and 52 (recall that $k_j > 0$ by convention) which must be removed.
- This is achieved by the scaling transformation:

$$C_{+j} = C'_{+j} e^{k_j \tau_t} \qquad \text{and} \qquad C_{-j} = C'_{-j} e^{-k_j \tau_b}. \tag{55}$$

Note that we have written:

- τ_t and τ_b for the optical depths at the top and the bottom of the layer, respectively.
- This was done deliberately to generalize this scaling scheme to apply to a multi-layered medium. In the present one-layer case we have $\tau_t = 0$ and $\tau_b = \tau^*$.

Light and Life Laboratory STEVENS Institute of Technology

Accurate Numerical Solutions (60)

Removal of Numerical Ill-Conditioning, cont....

Inserting eqns. 55 into eqns. 51 and 52 and solving for the C'_j instead of the C_j, we find that:

- All the exponential terms in the coefficient matrix have negative arguments ($k_j > 0, \tau_b > \tau_t$).
- Consequently, numerical ill-conditioning is avoided implying that the system of algebraic equations determining the C'_j will be unconditionally stable for arbitrary layer thickness.
- The merit of the scaling transformation is to remove all positive arguments of the exponentials occurring in the matrix elements of the coefficient matrix.

HOW DOES IT WORK?

Accurate Numerical Solutions (61)

- To demonstrate how this scheme works we shall use the two-stream case as an example:

Example: Removal of Ill-Conditioning – Two-Stream Case ($N = 1$)

In this simple case, eqns. 51 and 52 reduce to:

$$C_1 g_1(-\mu_1)e^{-k\tau_t} + C_{-1}g_{-1}(-\mu_1)e^{k\tau_t} = C_1 g_1^- e^{-k\tau_t} + C_{-1}g_{-1}^- e^{k\tau_t} = (RHS)_t$$

$$r_1 C_1 g_1(+\mu_1)e^{-k\tau_b} + r_{-1}C_{-1}g_{-1}(+\mu_1)e^{k\tau_b} = r_1 C_1 g_1^+ e^{-k\tau_b} + r_{-1}C_{-1}g_{-1}^+ e^{k\tau_b} = (RHS)_b$$

where we have used eqns. 27 and 28.

Light and Life Laboratory STEVENS Institute of Technology

Accurate Numerical Solutions (62)

The left hand side may be written in matrix form as:

$$\begin{bmatrix} g_1^- e^{-k\tau_t} & g_{-1}^- e^{k\tau_t} \\ r_1 g_1^+ e^{-k\tau_b} & r_{-1} g_{-1}^+ e^{k\tau_b} \end{bmatrix} \begin{bmatrix} C_1 \\ C_{-1} \end{bmatrix}.$$

This matrix is ill-conditioned because:

- One element becomes very large while another one becomes very small as $k\tau_b$ becomes large. This limits solutions to problems for which $k\tau_b < 3$ or 4.

Using the scaling transformation we find that the above matrix becomes:

$$\begin{bmatrix} g_1^- & g_{-1}^- e^{-k(\tau_b-\tau_t)} \\ r_1 g_1^+ e^{-k(\tau_b-\tau_t)} & r_{-1} g_{-1}^+ \end{bmatrix} \begin{bmatrix} C_1' \\ C_{-1}' \end{bmatrix}.$$

In the limit of large values of $k(\tau_b - \tau_t)$ this matrix becomes:

$$\begin{bmatrix} g_1^- & 0 \\ 0 & r_{-1} g_{-1}^+ \end{bmatrix}$$

Hence:

- **The ill-conditioning problem has been entirely eliminated.**

Light and Life Laboratory STEVENS Institute of Technology

Accurate Numerical Soln's – Inhomogeneous Slab (63)

So far we have considered only a homogeneous slab in which the single scattering albedo and the phase function were assumed to be constant throughout the slab. We shall now allow for both to be a function of optical depth:

- To approximate the behavior of a vertically inhomogeneous slab we will divide it into a number of layers. Thus:
- the slab is assumed to consist of L adjacent layers in which the single scattering albedo and the phase function are taken to be constant within each layer, **but allowed to vary from layer to layer.**
- For an emitting slab we assume that we know the temperature at the layer boundaries.
- The idea is that by using enough layers we can approximate the actual variation in optical properties and temperature as closely as desired.

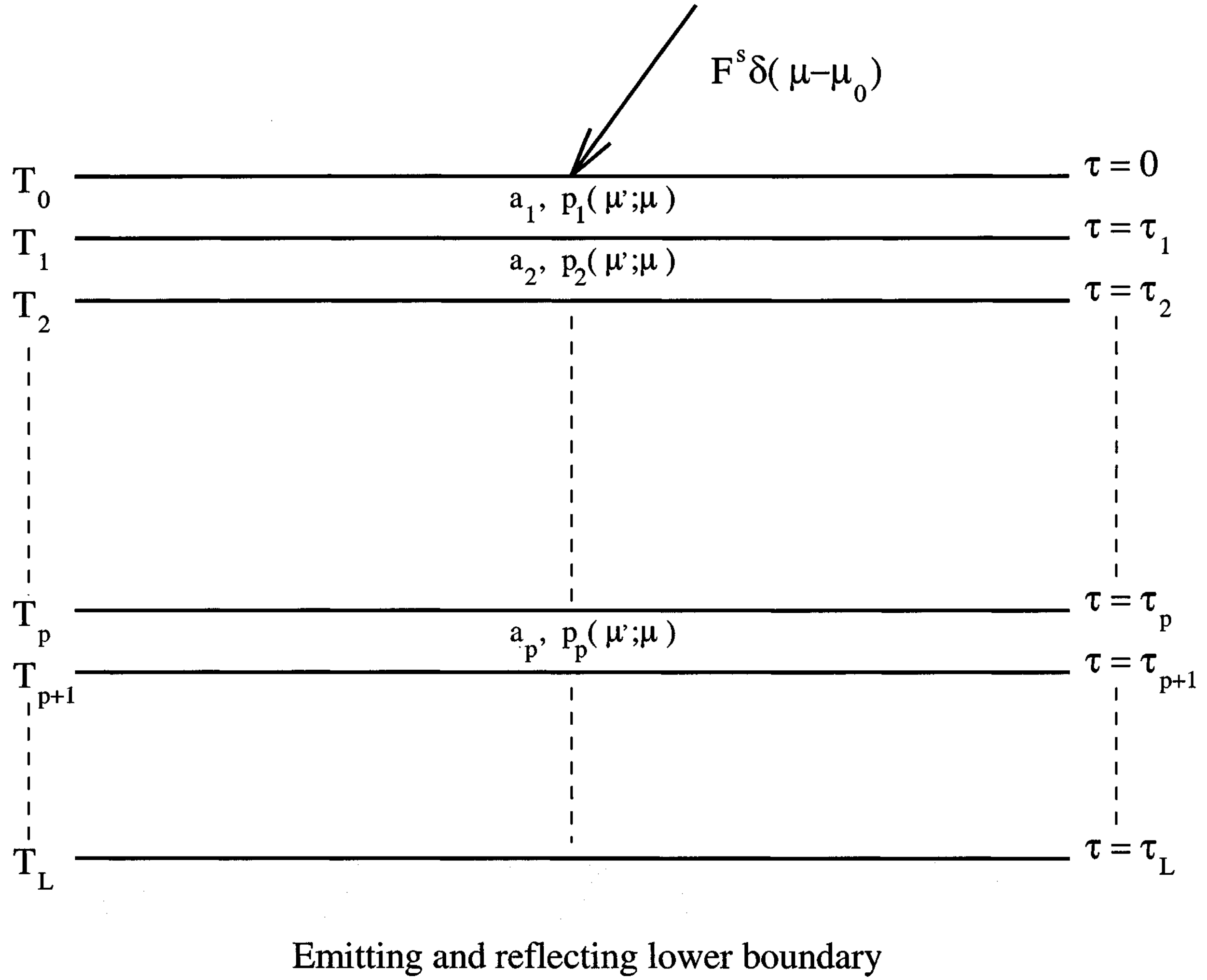

Figure 2: Schematic illustration of a multi-layered, inhomogeneous medium overlying an emitting and partially reflecting surface.

Accurate Numerical Soln's – Inhomogeneous Slab (65)

The advantage of this approach is that we can use the solutions derived previously because each of the layers by assumption is homogeneous.

- This implies that we may write the solution for the p^{th} layer as ($k_{jp} > 0$ and $k_{-jp} = -k_{jp}$)

$$I_p^{\pm}(\tau, \mu_i) = \sum_{j=1}^{N} \left[C_{jp} g_{jp}(\pm\mu_i) e^{-k_{jp}\tau} + C_{-jp} g_{-jp}(\pm\mu_i) e^{+k_{jp}\tau} \right] + U_p^{\pm}(\tau, \mu_i)$$
$$p = 1, 2, \ldots, L \qquad (56)$$

where

- the sum contains the homogeneous solution involving the unknown coefficients (the C_{jp}) and $U_p^{\pm}(\tau, \mu_i)$ is the particular solution given by eqn. 35.

Note that:

- except for the layer index p eqn. 56 is identical to eqn. 50 as it should be. The solution contains $2N$ constants per layer yielding a total of $2N \times L$ unknown constants.

Light and Life Laboratory STEVENS Institute of Technology

Accurate Numerical Soln's – Inhomogeneous Slab (66)

In addition to boundary conditions we must now require the intensity to be continuous across layer interfaces. As we shall see this will lead to a set of algebraic equations from which the $2N \times L$ unknown constants can be determined.

- Thus, eqn. 37 must now satisfy boundary and continuity conditions as follows:

$$I_1^m(0, -\mu_i) = \mathcal{I}^m(-\mu_i), \qquad i = 1, \ldots, N \tag{57}$$

$$I_p^m(\tau_p, \mu_i) = I_{p+1}^m(\tau_p, \mu_i), \qquad i = \pm 1, \ldots, \pm N;\ p = 1, \ldots, L-1 \tag{58}$$

$$I_L^m(\tau_L, +\mu_i) = I_s^m(\mu_i), \qquad i = 1, \ldots, N \tag{59}$$

where

- $I_s^m(\mu_i)$ is given by eqn. 49 with τ^* replaced by τ_L.
- Equation 58 is included to ensure that the intensity is continuous across layer interfaces.

Light and Life Laboratory STEVENS Institute of Technology

Accurate Numerical Soln's – Inhomogeneous Slab (67)

Insertion of eqn. 56 into eqns. 57–59 yields (omitting the m-superscript):

$$\sum_{j=1}^{N} \{C_{j1} g_{j1}(-\mu_i) + C_{-j1} g_{-j1}(-\mu_i)\} = \mathcal{I}(-\mu_i) - U_1(0, -\mu_i), \qquad i = 1, \ldots, N \tag{60}$$

$$\begin{aligned}\sum_{j=1}^{N} \{ & C_{jp} g_{jp}(\mu_i) e^{-k_{jp}\tau_p} + C_{-jp} g_{-jp}(\mu_i) e^{k_{jp}\tau_p} \\ & - \left[C_{j,p+1} g_{j,p+1}(\mu_i) e^{-k_{j,p+1}\tau_p} + C_{-j,p+1} g_{-j,p+1}(\mu_i) e^{k_{j,p+1}\tau_p}\right] \} = \\ & \qquad U_{p+1}(\tau_p, \mu_i) - U_p(\tau_p, \mu_i), \\ & \qquad i = \pm 1, \ldots, \pm N; p = 1, \ldots, L-1 \end{aligned} \tag{61}$$

$$\begin{aligned}\sum_{j=1}^{N} \left\{C_{jL} r_j(\mu_i) g_{jL}(\mu_i) e^{-k_{jL}\tau_L} + C_{-jL} r_{-j}(\mu_i) g_{jL}(\mu_i) e^{k_{jL}\tau_L}\right\} &= \Gamma(\tau_L, \mu_i), \\ i = 1, \ldots, N & \end{aligned} \tag{62}$$

where r_j is given by eqn. 53 with g_j replaced by g_{jL}, and Γ is given by eqn. 54 with $U^{\pm}$ replaced by $U_L^{\pm}$ and τ^* by τ_L.

Light and Life Laboratory STEVENS Institute of Technology

Accurate Numerical Soln's – Inhomogeneous Slab (68)

Equations 60–62 constitute:

- a $(2N \times L) \times (2N \times L)$ system of linear algebraic equations from which the $2N \times L$ unknown coefficients, the C_{jp} $(j = \pm 1, \ldots, \pm N; p = 1, \ldots, L)$ are determined.

Note that:

- eqns. 60 and 62 constitute the boundary conditions and are therefore identical to eqns. 51 and 52 (again except for the layer indices).
- As in the one-layer case we must deal with the fact that eqns. 60–62 are intrinsically ill-conditioned.
- Again, this ill-conditioning may be entirely eliminated by the scaling transformation introduced previously (eqns. 55). To illustrate how this scheme works for a multi-layered slab it suffices to consider two layers in the two-stream approximation.

Accurate Numerical Soln's – Inhomogeneous Slab (69)

In a multi-layered medium we may evaluate the integral in eqns. 38 and 39 by integrating layer by layer as follows ($\tau_{p-1} \leq \tau \leq \tau_p$ and $\mu > 0$):

$$\begin{aligned}\int_\tau^{\tau_L} \frac{dt}{\mu} S^+(t,\mu) e^{-(t-\tau)/\mu} &= \int_\tau^{\tau_p} \frac{dt}{\mu} S_p^+(t,\mu) e^{-(t-\tau)/\mu} \\ &+ \sum_{n=p+1}^{L} \int_{\tau_{n-1}}^{\tau_n} \frac{dt}{\mu} S_n^+(t,\mu) e^{-(t-\tau)/\mu} \end{aligned} \tag{63}$$

$$\begin{aligned}\int_0^{\tau} \frac{dt}{\mu} S^-(t,\mu) e^{-(\tau-t)/\mu} &= \sum_{n=1}^{p-1} \int_{\tau_{n-1}}^{\tau_n} \frac{dt}{\mu} S_n^-(t,\mu) e^{-(\tau-t)/\mu} \\ &+ \int_{\tau_{p-1}}^{\tau} \frac{dt}{\mu} S_p^-(t,\mu) e^{-(\tau-t)/\mu}. \end{aligned} \tag{64}$$

Accurate Numerical Soln's – Inhomogeneous Slab (70)

Using eqn. 41 for $S_n^{\pm}(t,\mu)$ in each layer (properly indexed) in eqns. 63 and 64, we find:

$$I_p^+(\tau,\mu) = I^+(\tau_L,\mu)e^{-(\tau_L-\tau)/\mu} + \sum_{n=p}^{L}\sum_{j=-N}^{N} C_{jn}\frac{\tilde{g}_{jn}(+\mu)}{1+k_{jn}\mu}[e^{-[k_{jn}\tau_{n-1}+(\tau_{n-1}-\tau)/\mu]} - e^{-[k_{jn}\tau_n+(\tau_n-\tau)/\mu]}] \quad (65)$$

with τ_{n-1} replaced by τ for $n = p$,

$$I_p^-(\tau,\mu) = I^-(0,\mu)e^{-\tau/\mu} + \sum_{n=1}^{p}\sum_{j=-N}^{N} C_{jn}\frac{\tilde{g}_{jn}(-\mu)}{1-k_{jn}\mu}[e^{-[k_{jn}\tau_n+(\tau-\tau_n)/\mu]} - e^{-[k_{jn}\tau_{n-1}+(\tau-\tau_{n-1})/\mu]}] \quad (66)$$

with τ_n replaced by τ for $n = p$. It is easily verified that for a single layer ($\tau_{n-1} = \tau$, $\tau_n = \tau_L = \tau^*$ in eqn. 65; $\tau_n = \tau$, $\tau_{n-1} = 0$ in eqn. 66) eqns. 65 and 66 reduce to eqns. 44 and 45 as they should.

Accurate Numerical Soln's – Inhomogeneous Slab (71)

Scaled Solutions

Equations 56 and 65 and 66 contain exponentials with positive arguments which will eventually lead to numerical overflow for large enough values of these arguments. Fortunately:

- we can remove all these positive arguments by introducing the scaling transformation into our solutions.

Since only the homogeneous solution is affected, it suffices to substitute eqns. 55 into the homogeneous version of eqn. 56 ignoring the particular solution $U_p^{\pm}(\tau, \mu_i)$:

$$I_p^{\pm}(\tau, \mu_i) = \sum_{j=1}^{N} \left\{ C'_{jp} g'_{jp}(\pm\mu_i) e^{-k_{jp}(\tau - \tau_{p-1})} + C'_{-jp} g_{-jp}(\pm\mu_i) e^{-k_{jp}(\tau_p - \tau)} \right\}. \qquad (67)$$

Since $k_{jp} > 0$ and $\tau_{p-1} \leq \tau \leq \tau_p$, all exponentials in eqn. 67 have negative arguments as they should to avoid overflow in the numerical computations.

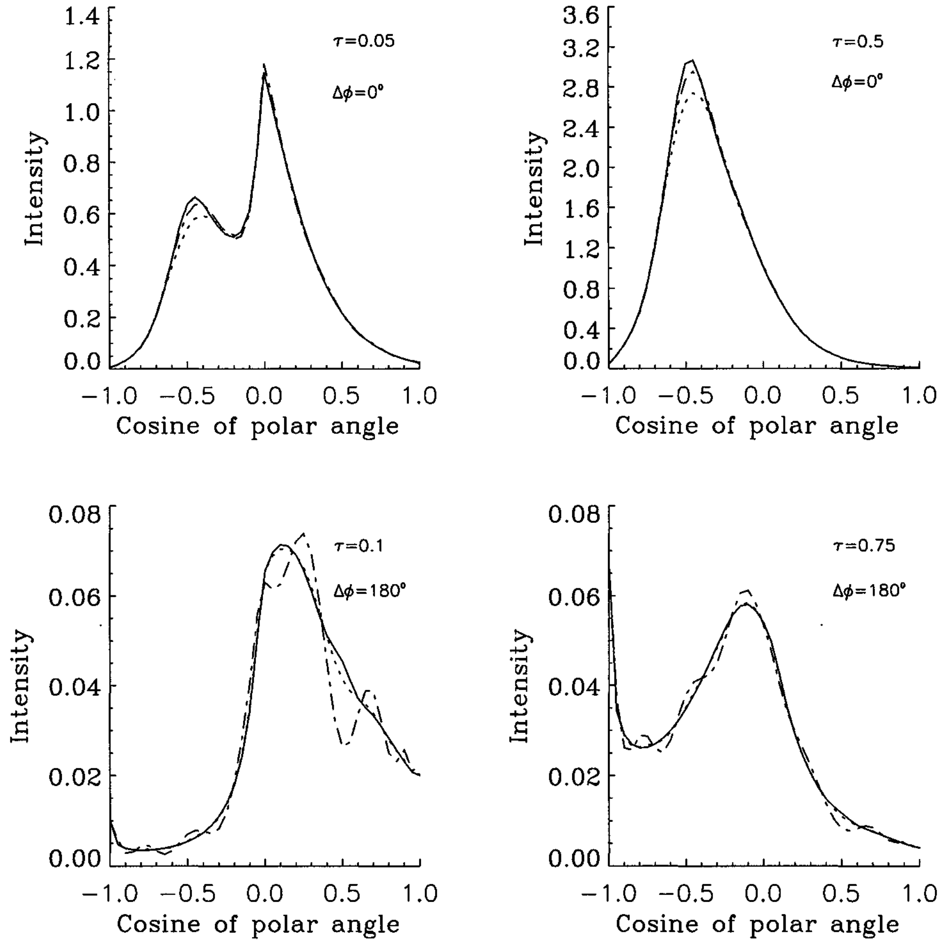

Figure 3: Comparison of accurate (48-stream) and approximate 16-stream diffuse intensities computed with and without $\delta - M$ scaling at several optical depths within an aerosol layer of total optical thickness $\tau_N = 1$ for $\Delta\phi = 0$, 90 and 180°. a=0.9, and $\mu_0 = -0.5$. Note that the ordinate scale is not the same in the various diagrams.

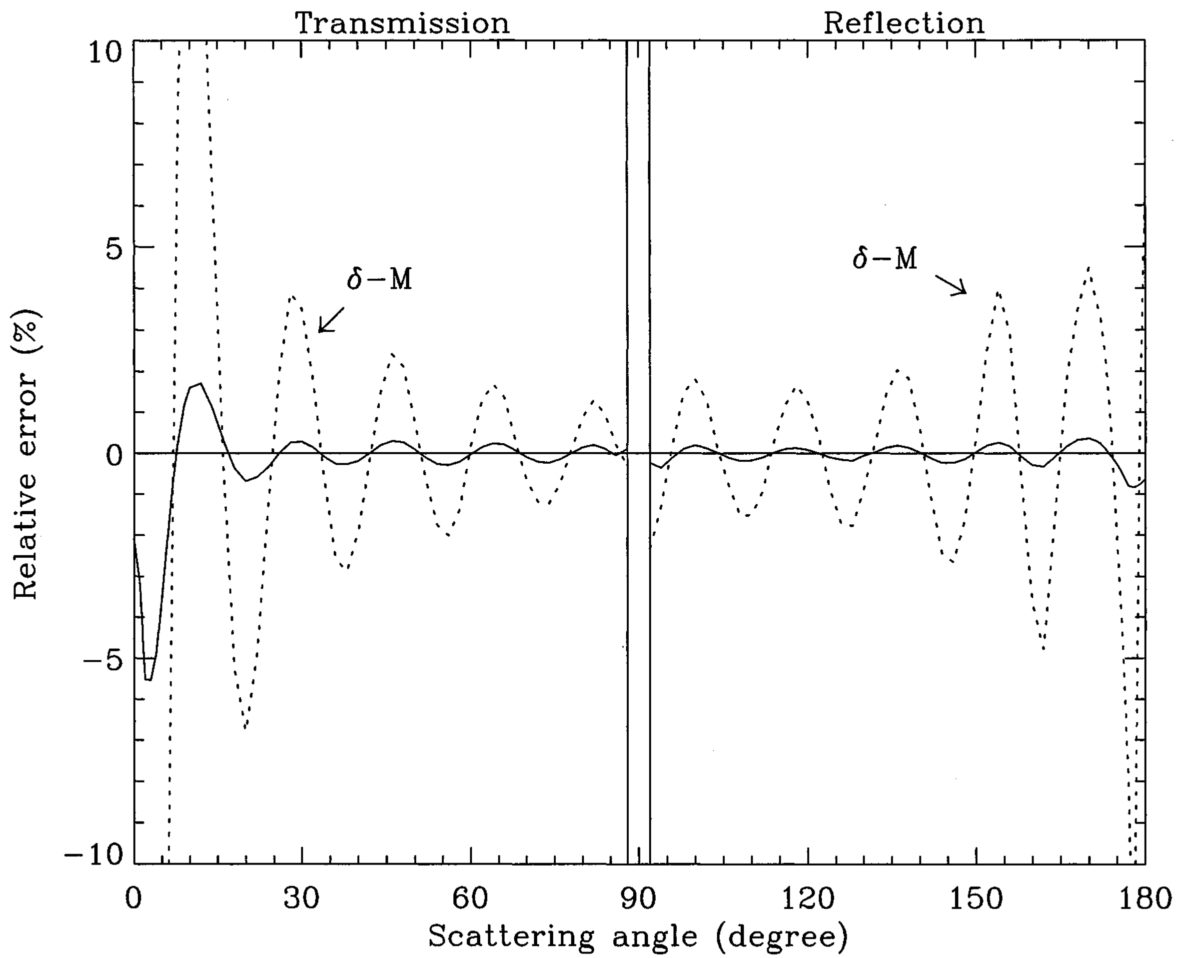

Figure 4: Relative error of the reflected and transmitted intensities computed by strict application of $\delta - M$ and by applying a correction to the $\delta - M$ method (solid line) which is simply the difference between the singly-scattered intensity computed from the exact phase function and fromthe $\delta - M$-scaled phase function. This example pertains to vertical (collimated) illumination of a homogeneous slab of total optical thickness 0.8 consisting of particles with scattering properties defined in the previous Figure.

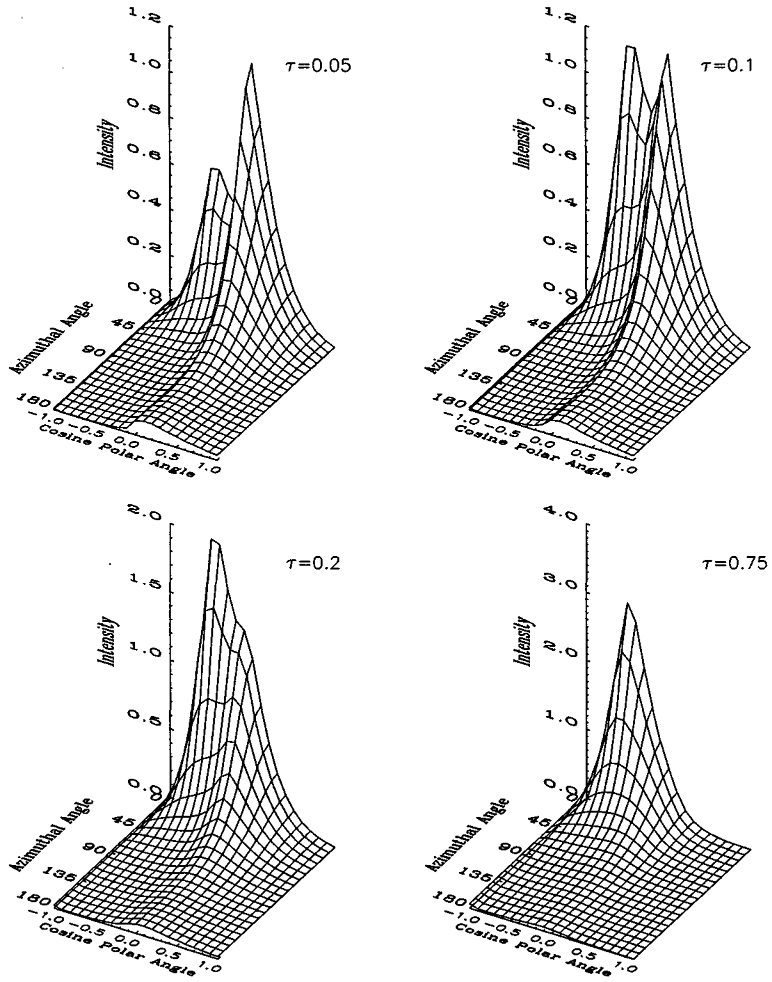

Figure 5: Three-dimensional display of diffuse intensity versus polar and azimuthal angles for several optical depths within a layer consisting of aerosol particles ('Haze L') of optical thickness $\tau_L = 1$, single scattering albedo $a = 0.9$, and cosine of solar zenith angle $\mu_0 = 0.5$.

Polarized Radiative Transfer Modeling

Knut Stamnes

Light and Life Laboratory

Department of Physics & Engineering Physcis

Arthur E. Imperatore School of Sciences Arts

Stevens Institute of Technology

Hoboken, NJ 07030

Light and Life Laboratory STEVENS Institute of Technology

Description of VDISORT

Brief History – 1

- The discrete ordinate radiative transfer algorithm (DISORT) has proven to be an accurate, versatile and reliable method for the solution of the scalar radiative transfer problem in plane-parallel, vertically inhomogeneous media.
- An extension of the scalar discrete ordinate theory to solve the 4-vector problem for the complete Stokes parameters was reported by Weng (1992), who adopted an approach to the solution of the vector problem completely analogous to the scalar case. Thus:
- the computer code for the vector problem could rely on the same well-tested routine to obtain the eigenvalues and eigenvectors as the one used in the scalar version (DISORT). Also:

Brief History – 2

- the same scaling transformation (Stamnes and Conklin, 1984) could be applied to circumvent the notorious ill-conditioning that occurs when applying boundary and layer interface continuity conditions.

The FORTRAN code developed by Weng had a few shortcomings:

- it had been applied exclusively in the microwave region, and thus had not been tested for beam source applications.
- the procedure to compute the Fourier component of the phase matrix turned out to be both inaccurate and inefficient.

To remove these flaws an improved version (Schulz et al., 1999):

- corrected errors in the numerical implementation
- replaced the procedure for computing the Fourier components of the phase matrix by a more accurate and efficient method
- tested the performance of the code against benchmark results.

Brief History – 2

However, although the code seems to have the potential to become an accurate and reliable tool for a variety of applications:

- no attempt has been made to test it in a systematic and comprehensive manner. Also, no attempt has been made to document the code thoroughly and extensively.

The original code provided solutions for the Stokes vector at the discrete ordinates (i. e. at the quadrature polar angles). Computer time increases cubically with the number of quadrature angles:

- **it becomes cost-effective to obtain the solution at a limited number of quadrature angles and then generate the solution at additional angles by using a much faster interpolation scheme.**

Brief History – 3

- Therefore, analytic expressions for the intensity at arbitrary angles and optical depths were developed for the vector code (Schulz and Stamnes, 2000).

WHY ARE THESE ANALYTIC EXPRESSIONS SO USEFUL? BECAUSE THEY SATISFY:

- **not only the radiative transfer equation, but also**
- **the boundary and layer-interface continuity conditions at arbitrary angles, and**
- **they have proven to be superior to standard interpolation schemes.**

Light and Life Laboratory
STEVENS Institute of Technology

Capabilities

The capabilites of the VDISORT code may be summarized as follows:

- It provides solutions for the Stokes vector at abritrary (user-specified) optical depths and at arbitrary (user-specified) polar angles.
- It can provide output at any number of layers and any number of angles in a single run at essentially no additional cost.
- It can be applied to compute the Stokes vector for ensembles of nonspherical particles (ice clouds).
- It can be applied to particles that are small compared to the wavelength (Rayleigh limit) as well as to particles in the Mie regime.
- It can be used to provide solutions for (solar) beam sources as well as internal (thermal emission) sources.

Light and Life Laboratory STEVENS Institute of Technology

Limitations

The current version of the code has the following limitations:

- It applies exclusively to plane-parallel geometry.
- The lower boundary is assumed to be a Lambertian reflector.
- Although the code has been tested for particles in the Mie regime, its performance has not been extensively tested for extreme phase matrices associated with ensembles of particles that are large compared to the wavelength.

FINAL THOUGHT/CHALLENGE:

- The speed of the DOM $\propto$ N^3: **its efficiency could probably be improved by constructing an eigensolver that takes full advantage of the fact that the eigenvalues are real!?)**

References

de Haan, J. F., P. B. Bosma, and J. W. Hovenier, (1987), The adding method for multiple scattering calculations of polarized light, Astron. Astrophys., 183, 371-391.

Dahlback, A., and K. Stamnes, (1991), A new spherical model for computing the radiation field available for photolysis at twilight, Planet. Space Sci., 39, 671-683.

Frette, O., J. J. Stamnes, and K. Stamnes, Optical remote sensing of marine constituents in coastal waters: A feasibility study, Applied Optics, 37, 8218-8326, 1998.

Frette, O., S. R. Erga, J. J. Stamnes, and K. Stamnes, Optical remote sensing of waters with vertical structure, Applied Optics, 40, 1478-1487, 2001.

Light and Life Laboratory STEVENS Institute of Technology

Hu, Y.-X., B. Wielicki, B. Lin, G. Gibson, S.-C. Tsay, K. Stamnes, and T. Wong, (2000), Delta-fit: A fast and accurate treatment of particle scattering phase functions with weighted singular-value decomposition least squares fitting, J. Quant. Spectrosc. Radiat. Transfer, 69, 681-690.

Levoni, C., E. Cattani, M. Cervino, R. Guzzi, W. Nicolantonio, Effectiveness of the MS-method for computation of the intensity field reflected by a multi-layer plane-parallel atmosphere, J. J. Quant. Spectrosc. Radiat. Transfer, 69, 635-650, 2001.

Nakajima, T. and M. Tanaka, Algorithms for radiative intensity calculations in moderately thick atmospheres using a truncation approximation, J. Quant. Spectrosc. Radiat. Transfer, 40, 51-69, 1988.

Schulz, F. M., K. Stamnes, and F. Weng, (1999), VDISORT: An improved and generalized discrete ordinate radiative transfer model for polarized (vector) radiative transfer computations, J. Quant. Spectrosc. Radiat. Transfer, 61, 105-122.

Schulz, F. M., and K. Stamnes, (2000), Angular distribution of the

Stokes vector in a plane parallel, vertically inhomogeneous medium in the vector discrete ordinate radiative transfer (VDISORT) model, J. Quant. Spectrosc. Radiat. Transfer, 65, 609-620.

Spurr, R. D. J., T. P. Kurosu, and K. V. Chance, (2001), A linearized discrete ordinate radiative transfer model for atmospheric remote sensing retrieval, J. Quant. Spectrosc. Radiat. Transfer, 68, 689-735.

Stamnes, K., (1982), On the computation of angular distributions of radiation in planetary atmospheres, J. Quant. Spectrosc. Radiat. Transfer, 28, 47-51.

Stamnes, K. and P. Conklin, (1984), A new multi-layer discrete ordinate approach to radiative transfer in vertically inhomogeneous atmospheres, J. Quant. Spectrosc. Radiat. Transfer, 31, 273-282.

Stamnes, K., S.-C. Tsay, W. J. Wiscombe, K. and Jayaweera, (1988), Numerically stable algorithm for discrete-ordinate-method radiative transfer in mutiple scattering and emitting layered media, *Appl. Opt.*, **27**, 2502-2509.

Stamnes, K., S.-C. Tsay, W. J. Wiscombe and I. Laszlo, (2000), DISORT, a General-Purpose Fortran Program for Discrete-Ordinate-Method Radiative Transfer in Scattering and Emitting Layered Media: Documentation of Methodology, Report, available from ftp://climate.gsfc.nasa.gov/pub/wiscombe/Multiple Scatt/.

Thomas, G. E. and K. Stamnes, (1999), Radiative Transfer in the Atmosphere and Ocean, *(Cambridge University Press)*.

Weng, F., (1992), A multi-layer discrete-oridinate method for vector radiative transfer in a vertically-inhomogeneous, emitting and scattering atmosphere–I. Theory. J. Quant. Spectrosc. Radiat. Transfer, 47, 19-33.

Wiscombe, W. J., (1977), The delta-M method: Rapid yet accurate radiative flux calculations for strongly asymmetric phase functions, J. Atmos.

Yan, B., K. Stamnes, W. Li, B. Chen, J. J. Stamnes, and S. C. Tsay, Pitfalls in atmospheric correction of ocean color imagery: How should aerosol optical properties be computed?, Applied Optics, in press,

2001. Sci., 33, 1408-1422.